ZEUS Note 94-167

Determination of the ZEUS Luminosity in '93

Krzysztof Piotrzkowski Maciej Zachara

Institute of Nuclear Physics,
Kraków, Poland

Luminosity Monitor Group

January 5, 1995

Abstract

History the '93 luminosity measurement and the algorithms of the luminosity calculations are described. Detailed discussion of the systematic errors is presented and final results are reported.

1 Introduction

The idea of monitoring HERA luminosity by the measurement of high-energy ep bremsstrahlung events proved to be quite successful. HERA beams induced less background than expected which was not disturbing seriously bremsstrahlung measurement. This left a very high event rate ($> 10^5$ events/s) as a main experimental challenge in the luminosity measurement. Initially, the measurement was thought as a kind of coincidence counting experiment, where energy measurement is not so relevant and results are determined mainly by the geometry of the experimental setup. This idea was actually dropped in favor of single rate measurements where precise energy measurement is essential. This note reports on the second year (1993) of the luminosity measurement in ZEUS.

2 Running Condition

2.1 HERA Performance

In the 1993 running period HERA provided luminosity for experiments from the end of June till the end of October. Initially the bunch structure of the beams (with 10 colliding bunches) was the same as in '92. Then, after a few days of running, HERA was switched to a new operation mode with 84 colliding bunches (plus 10 electron and 6 proton pilot bunches) which allowed to reach higher luminosities. Colliding bunches were stored in 10-bunch trains plus a single 4 bunch train while the electron pilot bunches were circulating in pairs.

The most important parameters which characterize the HERA performance in 1993 are shown in Figs. 1,2,3,4 as a function of the ZEUS run number. A big progress achieved by HERA during the running period can be clearly seen. Both the specific and instantaneous luminosity were steadily improving. The typical beam currents at injection increased for both beams from a few mA in July up to 15 mA in the last two months of the 1993 operation. The maximum instantaneous luminosity reached $\approx 1.5 \times 10^{30} cm^{-2}s^{-1}$, i.e. 10% of the design value. The observed maximum specific luminosity, $\approx 7.5 \times 10^{29} cm^{-2}s^{-1}mA^{-2}$, was even higher than expected.

2.2 Luminosity Monitor Operation

The priciples the luminosity measurement in ZEUS and the experimental setup of the luminosity monitor have been described elsewhere [1, 2], here we will briefly describe only their basic features.

The luminosity determination is based on the detection of the ep bremsstrahlung events. Initially, the events were identified by detection in coincidence of a scattered electron and a radiated photon. It was found however that the accuracy of the measurement is seriously limited by poor understanding of an electron acceptance. So, in summer 1992 it was decided to use only hard bremsstrahlung photons for the luminosity measurement.

The photon detector in the luminosity monitor consisted of a copper exit window from a proton beam-pipe at 82 m from the interaction point (IP), a carbon filter of the variable

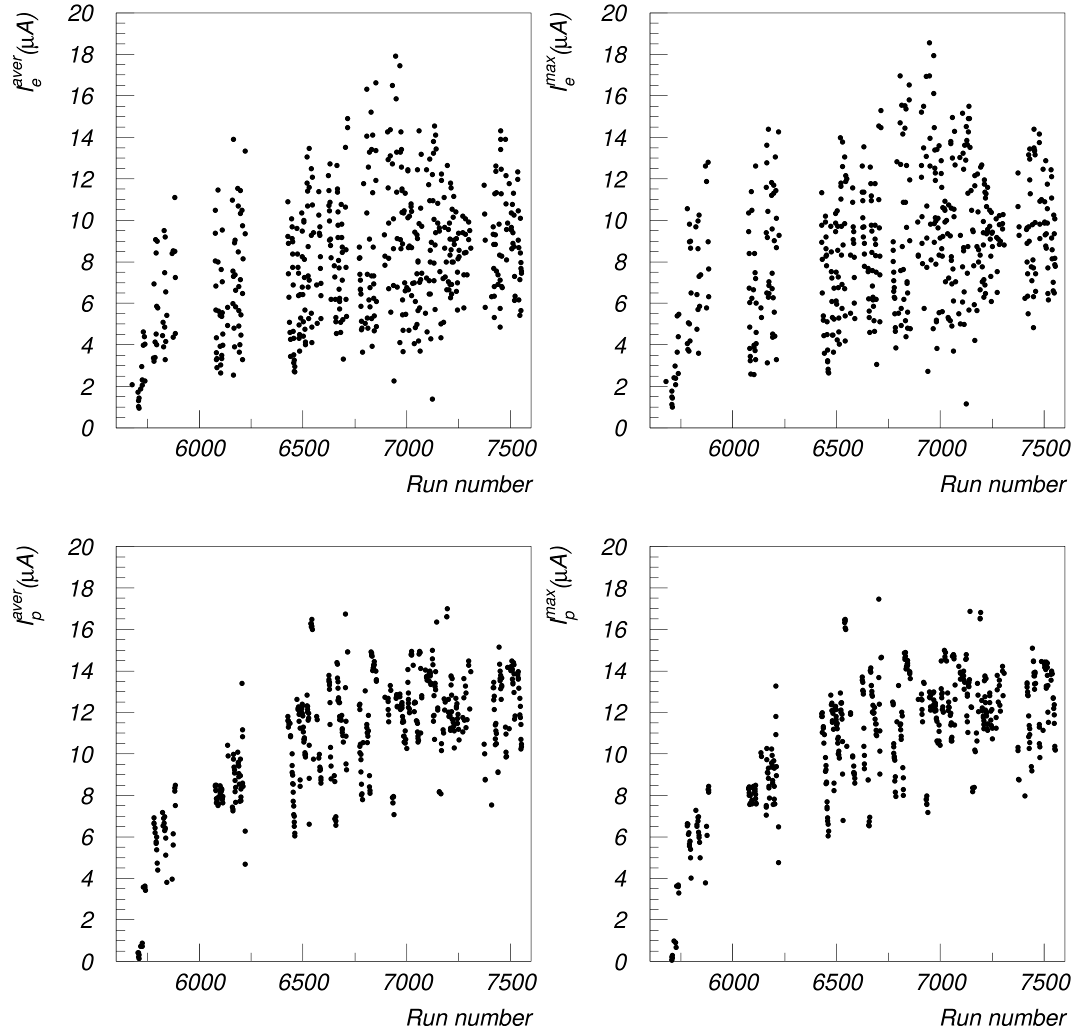

Figure 1: HERA performance: Average and maximum beam currents as a function of the ZEUS run number.

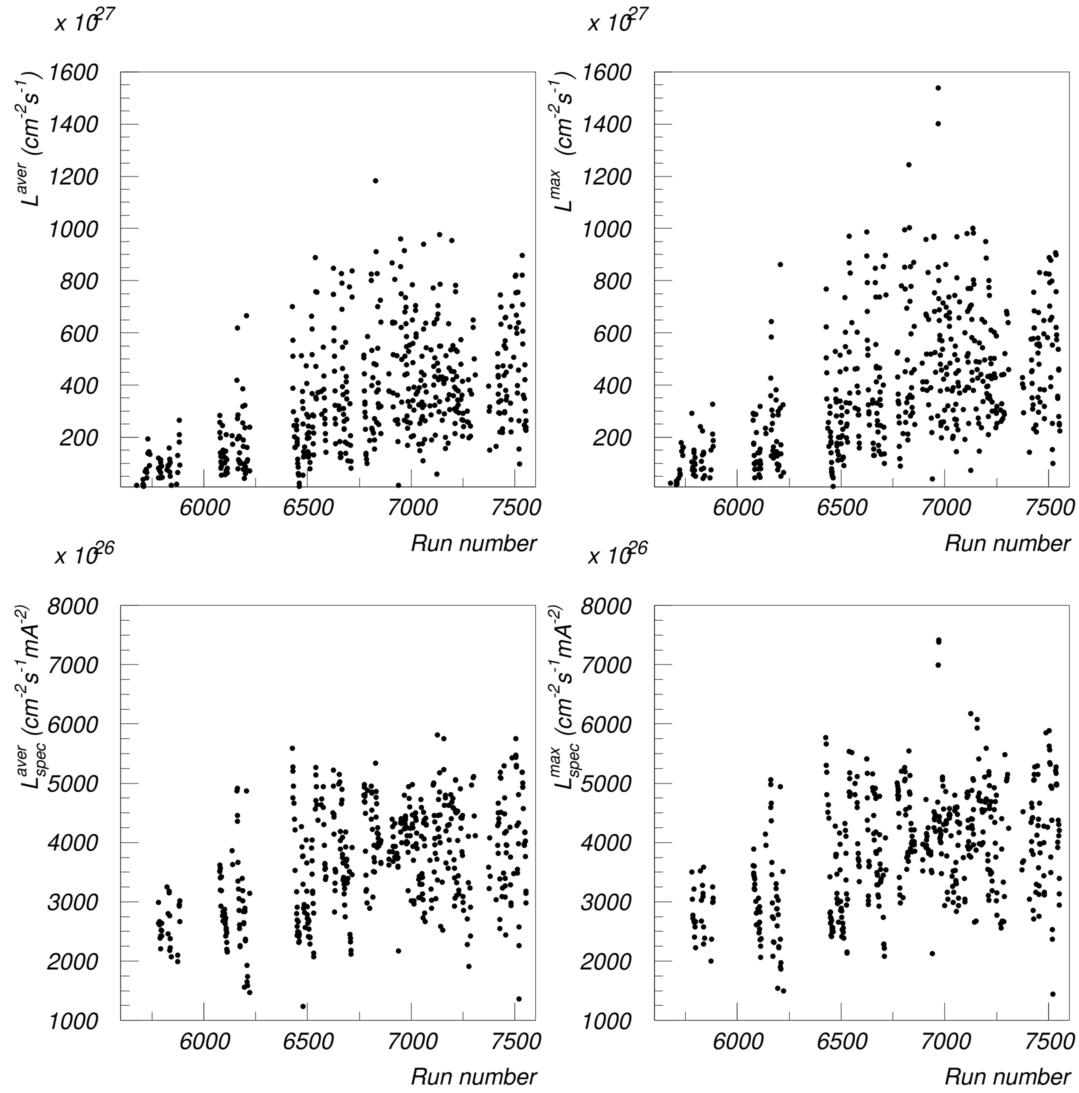

Figure 2: HERA performance: Average and maximum instantaneous and specific luminosities as a function of the ZEUS run number.

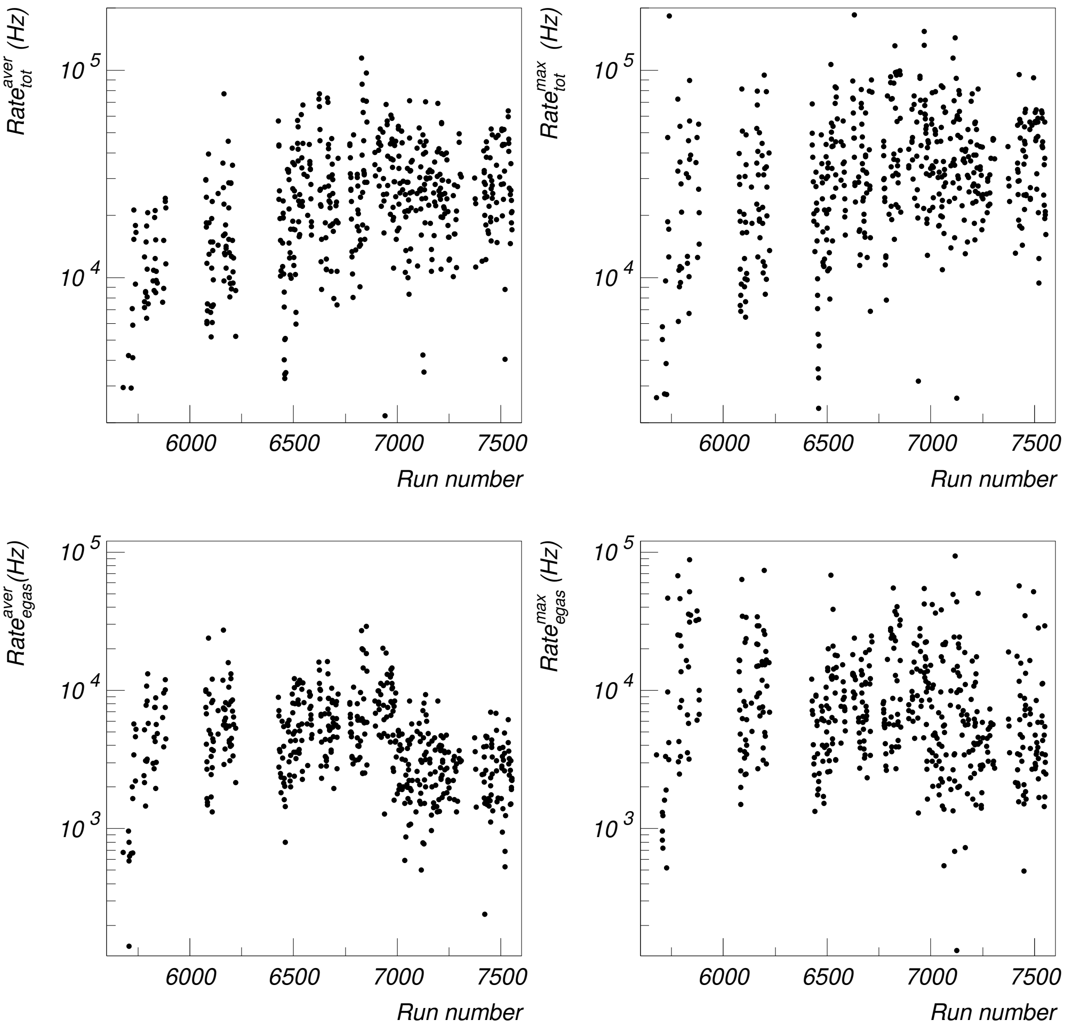

Figure 3: HERA performance: Average and maximum bremsstrahlung rates (total and $egas$) for the $E_\gamma > 5\ GeV$ trigger as a function of the ZEUS run number.

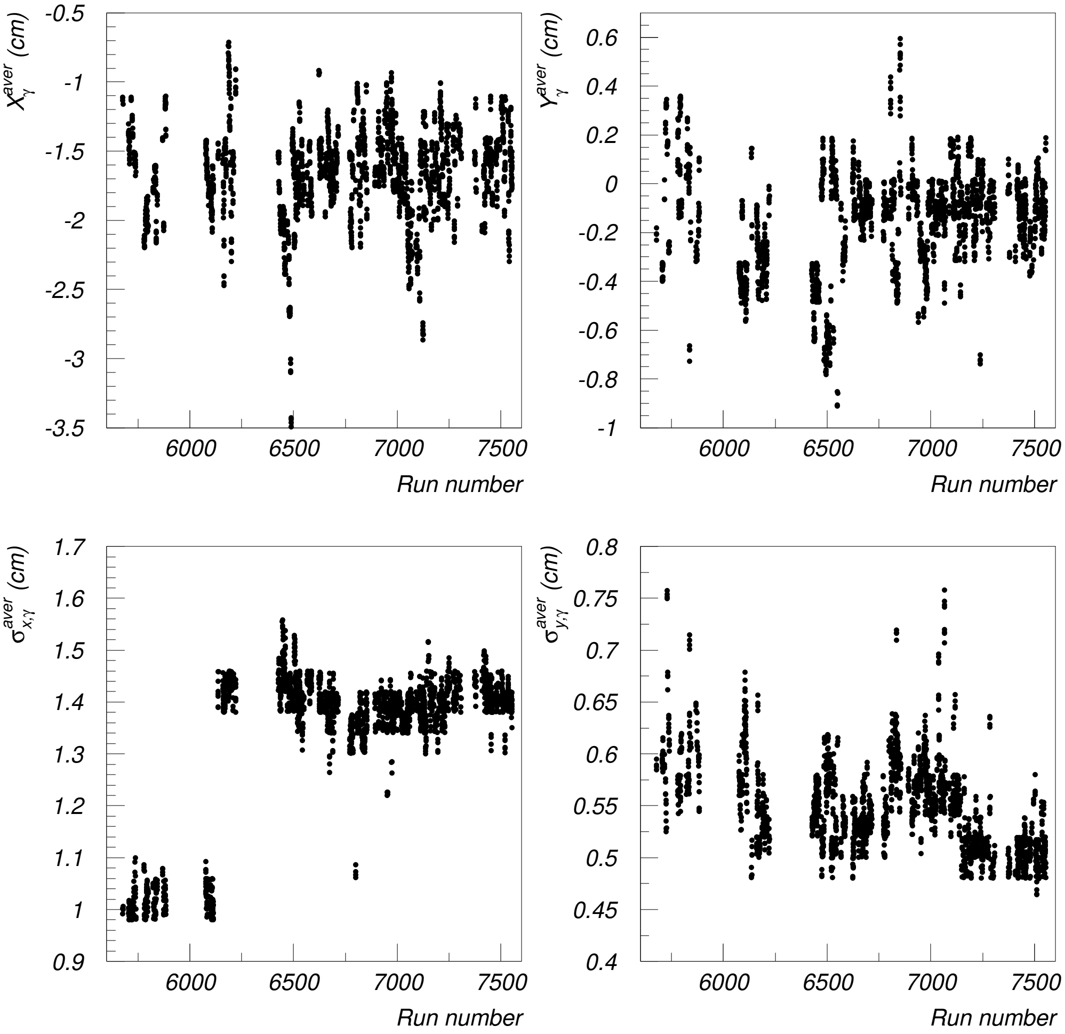

Figure 4: HERA performance: Average positions and widths of the photon beam at γcal as a function of the ZEUS run number.

thickness (0.5–3.5 *radiation lengths*, r.l.) at about 103 m from the IP, used as a shielding against the synchrotron radiation, followed by a 24 r.l. deep lead-scintillator electromagnetic calorimeter at 106 m from the IP. Inside the calorimeter at the depth of 7 r.l. a position detector consisting of two crossed layers of scintillator fingers was installed.

The position detector helped to understand the acceptance of the bremsstrahlung as well as to optimize conditions of the measurement by steering photon beam to the position of maximum efficiency of photon detection.

The existence of the carbon filter, unavoidable due to the huge flux of direct synchrotron photons, spoiled the energy resolution of the photon calorimeter since the majority of the bremsstrahlung photons interacted in the filter before reaching it. The original setup had included a Čerenkov counter installed between the filter and the calorimeter which could veto events when a high energy photon interacted in the filter. Vetoing efficiency of the counter was however poorly controlled therefore it was not used for identification of 'luminosity events' already in 1992 and in the 92/93 winter shutdown was eventually removed from the HERA tunnel.

Both, the detectors and the data acquisition system were performing during the 1993 running period quite reliably. The operation of the luminosity monitor was somehow disturbed by unexpectedly high sensitivity of gain of the calorimeter photomultipliers to the mean anode current (see [3]). This effect deteriorated primarily the on-line luminosity measurement where the recalibration of the readout channels was not performed. It complicated also off-line analysis because often the gains changed significantly during a single long run, and the data samples had to be split into pieces and analyzed separately.

The rate of bremsstrahlung events was measured for the online luminosity determination with the use of scalers in the LUMI local VME based system. Separate scalers measured total rate and the rate of events corresponding to pilot bunches. In 1993 the online measurement was based on the detection of photons with energies higher than 49 ADC counts (equivalent to 5 GeV threshold for nominal conditions).

The offline luminosity determination was based on data contained in the ZEUS so-called *environmental* records. A program using this data was submitted on DESY IBM main-frame computer separately for each ZEUS physics run. Environmental data include readouts from the scalers used for the online measurement and from additional 96 scalers available in the ZEUS first-level trigger system (GFLT). 32 GFLT scalers counted bremsstrahlung events satysfing eight different cuts on the photon and/or electron energies. For each type of the cut four scalers were available counting events for all bunches and electron pilot bunches with and without dead-time correction. Additional 64 scalers were counting bremsstrahlung events separately for 64 bunch crossing numbers (BCN). Other information stored in environmental records as time stamps, elapsed trigger dead time, beam currents and data provided by detectors of the luminosity monitor (energies, positions) were also used in the offline analysis. The offline procedure started relatively late in 1993 since it needed the calorimeter calibration constants and pedestal values separately for each ZEUS run. There were only a few short runs for which the offline procedure failed due to environmental data being non-valid. The integrated luminosity for those runs was about 0.01% of the total 1993 ZEUS luminosity.

3 Luminosity Determination

3.1 Introduction

The luminosity is defined by the formula:

$$R = \mathcal{L}\ \sigma, \tag{1}$$

where R is the event rate of the process which has a cross-section σ and $\mathcal{L}$ is the luminosity. One can use this formula for the luminosity measurement provided that the cross-section is well known and the event rate can be precisely measured. The bremsstrahlung process $ep \to ep\gamma$ has been chosen for the luminosity measurement at HERA because it has a large cross section known from QED and a clean experimental signature. The ZEUS luminosity monitor can detect with high efficiency both the scattered electron and radiated photon. The bremsstrahlung differential cross section $d\sigma_{BH}/dE_\gamma$ is given (in Born approximation) by the Bethe-Heitler formula [4], which for high energy ep collisions reads:

$$\frac{d\sigma_{BH}}{dE_\gamma} = 4\alpha r_e^2 \frac{E'_e}{E_\gamma E_e}(\frac{E_e}{E'_e} + \frac{E'_e}{E_e} - \frac{2}{3})(ln\frac{4E_pE_eE'_e}{MmE_\gamma} - \frac{1}{2}), \tag{2}$$

where:
E_γ - photon energy,
E_e, E'_e - energy of primary and secondary electrons,
E_p - proton energy,
M, m - proton and electron masses,
α - fine structure constant,
r_e - classical electron radius.

Experimentally, luminosity was calculated from the rate of ep bremsstrahlung events R_{ep} and the luminosity definition formula:

$$\mathcal{L} = \frac{R_{ep}}{\sigma_{obs}}. \tag{3}$$

Unfortunately, bremsstrahlung of beam electrons on the rest gas molecules has an even larger cross-section ($\sigma \sim Z^2$ to good approximation, where Z is an electric charge of the nucleus) and, since it has the same experimental signature as the ep bremsstrahlung, it represents a severe background. This background was statistically subtracted using electron pilot bunches, so R_{ep} was the rate obtained from the observed total rate of bremsstrahlung events after correction for the electron-gas ($egas$) contribution:

$$R_{ep} = R_{tot} - kR_{pilot}, \tag{4}$$

where: R_{tot} is the total rate of the bremsstrahlung events, R_{pilot} is the rate measured for the electron pilot bunches and k is the ratio of the total electron current to that in the pilot bunches. The observed cross-section σ_{obs} can be written generally in the form:

$$\sigma_{obs} = \int A_{lumi} d\sigma_{BH} \tag{5}$$

Table 1: Number of MC luminosity events and the corresponding 'observed' cross-sections, σ_{obs}, for 26.67 GeV electron and 820 GeV proton beam energies and for four photon trigger types.

Trigger type	Number of events	σ_{obs}
$E_\gamma > 28(2\ GeV)$	60591.0	119.63 mb
$E_\gamma > 49(5\ GeV)$	34616.0	68.35 mb
$E_\gamma > 84(10\ GeV)$	18780.2	37.08 mb
$127 > E_\gamma > 84(16, 10\ GeV)$	9414.2	18.59 mb

where A_{lumi} is a probability that a bremsstrahlung event will be identified as a luminosity event and integration is over the whole relevant range of photon four-momenta.

3.2 Monte Carlo Simulation

For the simulation of the luminosity detector the MOZART version 10v3 was used and the BREMLU [5] program for generating ZDIS events. Two MC data samples were produced for 26.67 GeV electron and 820 GeV proton beam energies: 49662 ep bremsstrahlung events with photon energies in the range $26.66 > E_\gamma > 3GeV$ and 49820 ep bremsstrahlung events in the range $3 > E_\gamma > 0.1GeV$. A final MC sample containing 165259 entries with bremsstrahlung photon energy in the $26.66 > E_\gamma > 0.1GeV$ range was created by weighting the low energy sample as to match the ratio of bremsstrahlung cross-sections corresponding to two energy sub-intervals. Since the cross-section for the full range $26.66 > E_\gamma > 0.1GeV$ is 326.30mb the sample corresponds to an integrated luminosity of 0.506 μb^{-1}. Simulation with MOZART provided energy deposits in the calorimeter scintillator plates corrected for the light attenuation, and two scintillator readout values, for up and down WLS plates. Then the MOZART (up and down) readouts were converted to ADC counts with the use of a factor converting the energy deposits to the measured photon energy (found to be 1/0.020 with the same technique which was used for data calibration [3]) and the nominal parameters: two pedestals equaled 15 ADC counts and two ADC calibration constants equaled 7 ADC counts per 1 GeV photon energy. Finally, an arithmetic average of the two ADC readouts was taken.

For the simulation of the data send to the GFLT, some migration of events had to be added. It accounted for a bug (bad connection) present in a LUMI GFLT board in '93 running period and causing migration of about 80% events from even bins to bins one channel up, see Fig. 5.

Then, by applying the same cuts (in ADC counts) which were used for flagging luminosity events, the number of triggered luminosity events and corresponding 'observed' cross-sections were found as shown in Tab. 1.

There were however some more corrections applied. The first correction was due to unequal FADC bin widths. The actual sizes of the FADC bin widths were measured by scanning 8-bit FADC inputs with DC voltage provided by a 12-bit DAC. In such a way a bin width map could be calculated as well as a running sum of the bin widths (see Fig. 7) [6]. This effect shifted luminosity trigger thresholds up and down in energy and had to be corrected for.

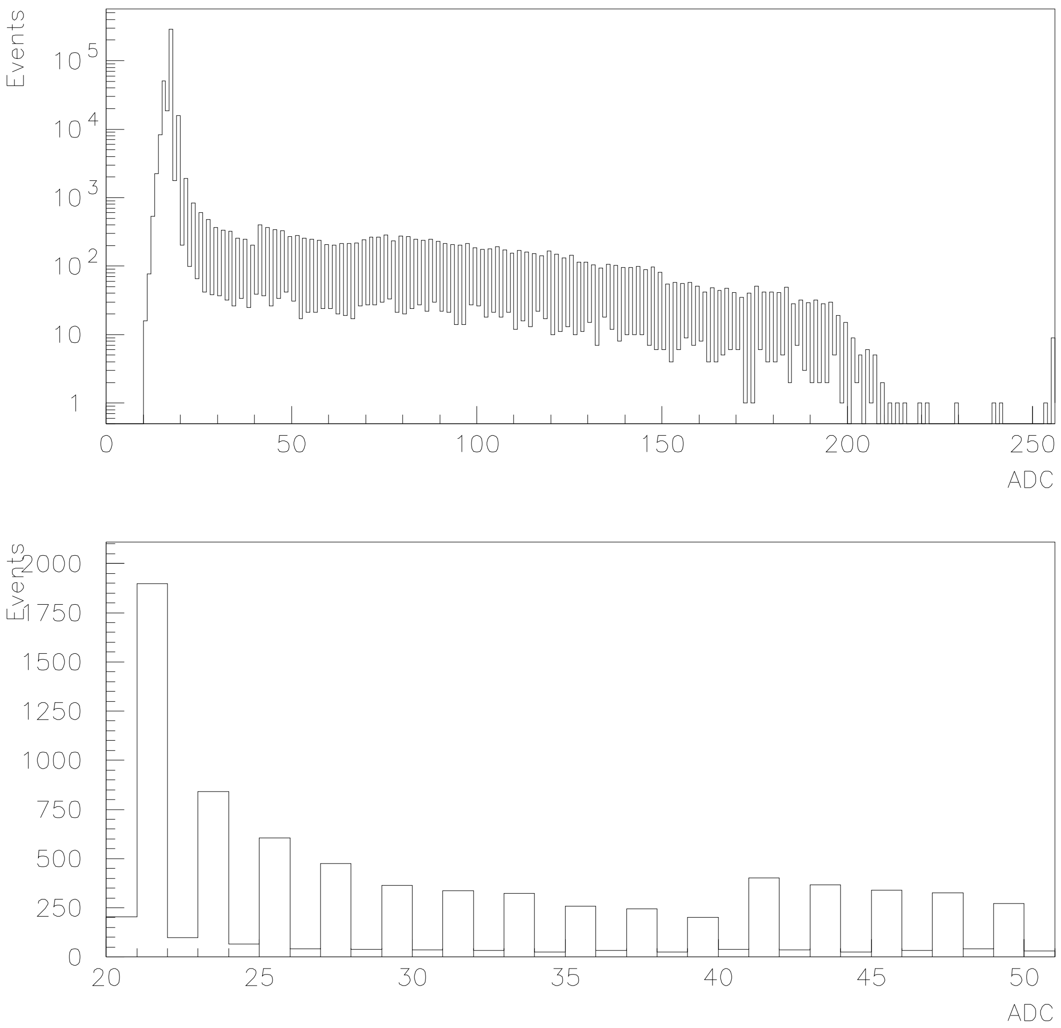

Figure 5: LUMI photon energy spectrum in ADC counts from a GFLT on-line histogram file.

The second correction was due to the change of the Bethe-Heitler ep cross-section when the finite lateral beam sizes at HERA were taken into account. The correction was simulated in the MC with the use of the BREMGE generator which fairly well describes theoretical predictions [7].

The third correction was due to the use of the ADC pedestals provided by the calorimeter calibration procedure [3] where the pedestals were determined separately for each ADC channel. Because in the luminosity measurement an average of two ADC counts is used, therefore the pedestal should be also calculated for the average of two readouts. Such a pedestal was usually 0.25 ADC counts lower than an average of two separate ADC pedestals [1].

The next correction was due to non-linearity of the readout electronics, most probably non-linearity of phototubes working at low voltages (700-800 V – to avoid large anode currents), as was suggested in [3] and was consistent within large errors with fit results for the $egas$ bremsstrahlung spectrum (see Fig. 6). The parametrization of the non-linearity in photon measurement is given by the calibration method [8]: $E_{meas} = E_{true}(1 + f_{nonlin} * (E_{beam} - E_{true}))$, where E_{meas}, E_{true} are measured and true photon energy, E_{beam} is an electron beam energy where the photon calorimeter had been calibrated and f_{nonlin} is a non-linearity factor. Recently, it was directly measured with the use of LED test system [9] and found to be $0.06 - 0.07\%/GeV$ [2]. However, no such measurement was performed in '93.

The last correction was due to pileup of more than one bremsstrahlung event in a single beam collision. The pileup effect can increase the rate of the luminosity events when the dominating mechanism is that two (or more) non-luminosity events make up together one luminosity event. The rate decreases when pileup of two or more luminosity events dominates and one counts one 'good' event instead of two, for example. The pileup corrections are to a high accuracy linear functions of the event rates, i.e. the effect is mainly due to double events.

All above corrections as well as final cross-sections (without pile-up correction which has to be corrected on a run-to-run basis) are listed in Tab. 2.

3.3 Online Procedure

Online calculations were done using the main LUMI scalers and the bunch currents data - ep bremsstrahlung rate was calculated from Eq. 4 and luminosity was obtained by multiplying the rate with a factor of $1.49 \times 10^{25} cm^{-2} s^{-1}$ corresponding to the σ_{obs}^{-1} for the nominal conditions.

Fig. 8 shows the uncorrected integrated online luminosity measured with the ZEUS luminosity monitor for the physics runs in 1993. To obtain the luminosity corresponding to the data sample taken with ZEUS one has to take into account also the deadtime of the ZEUS data acquisition system. It was done indirectly by the ZEUS main Run Control programs. It appeared that this correction was not always correct, especially for runs with high deadtime,

[1] It is due to rounding in an integer average of two ADC counts, which shifts the result by 0.5 in about 50% of events.

[2] It was done by measurement of the LED signal with calorimeter photomultipliers for several slightly different HVs (in one per cent steps) and for several fixed intensities of a LED pulse. The ratios between measured signals for different LED pulses should not depend on HV. The deviation from constant behaviour was used as a measure of non-linearity.

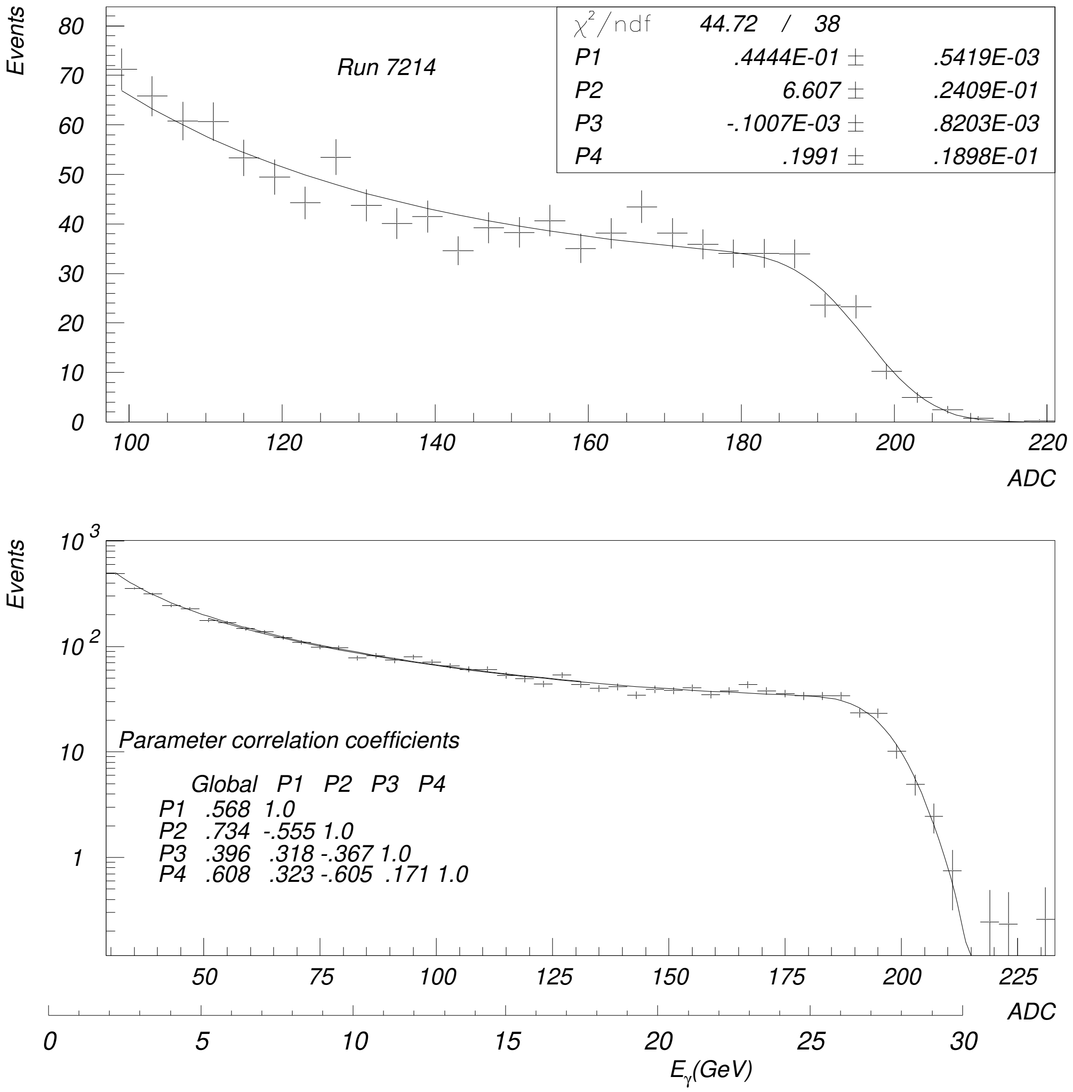

Figure 6: The measured $egas$ bremsstrahlung spectrum in run 7214 with fitted Bethe-Heitler shape smeared with Gaussian resolution of the photon calorimeter and distorted by non-linearity term; fitted parameters are: P1 - normalization, P2 - γcal calibration constant, P3 - non-linearity factor f_{nonlin}, P4 - energy resolution at 1 GeV.

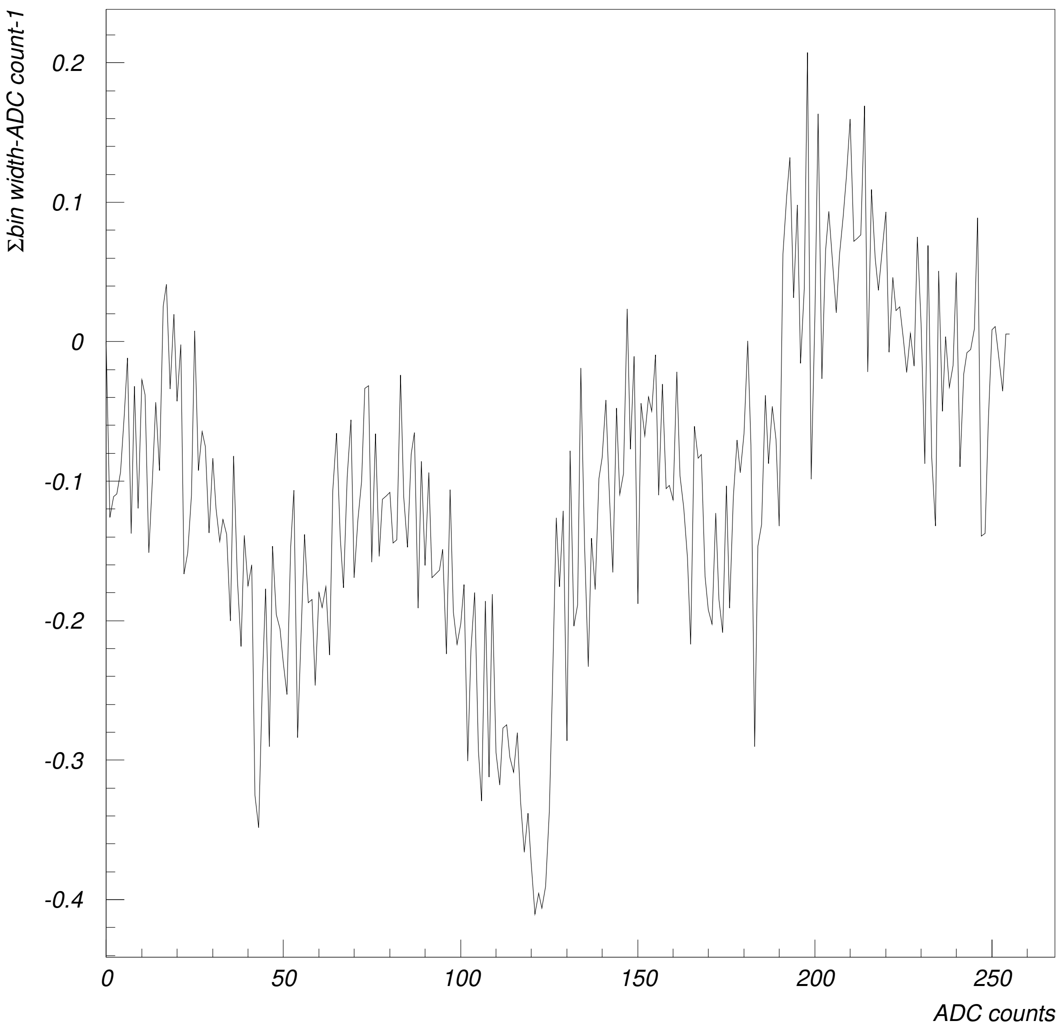

Figure 7: The distribution of the difference between a measured and expected running sum of bin widths (=$\Sigma bin\ width$–ADC count–1) as a function of FADC channel number.

Table 2: Corrections to MC 'observed' cross-sections (pileup correction corresponds to $5 \times 10^{29} cm^{-2}s^{-1}$ luminosity and 20% of $egas$ background) and final 'observed' cross-sections.

Correction	Trigger type			
type	$E_\gamma > 28$	$E_\gamma > 49$	$E_\gamma > 84$	$127 > E_\gamma > 84$
FADC threshold value	+0.07%	+0.22%	–0.08%	–0.45%
Beam size effect	–2.0%	–0.9%	–0.25%	–0.5%
Pedestal shift	–0.9%	–0.5%	–0.4%	–0.3%
Non-linearity in electronics	+0.95%	+1.2%	+1.4%	+1.2%
Final σ_{obs}	117.38 mb	68.36 mb	37.33 mb	18.58 mb
Event pile-up ($\mathcal{L} = 5 \times 10^{29} cm^{-2}s^{-1}$)	–0.75%	0.0%	+0.6%	–0.3%

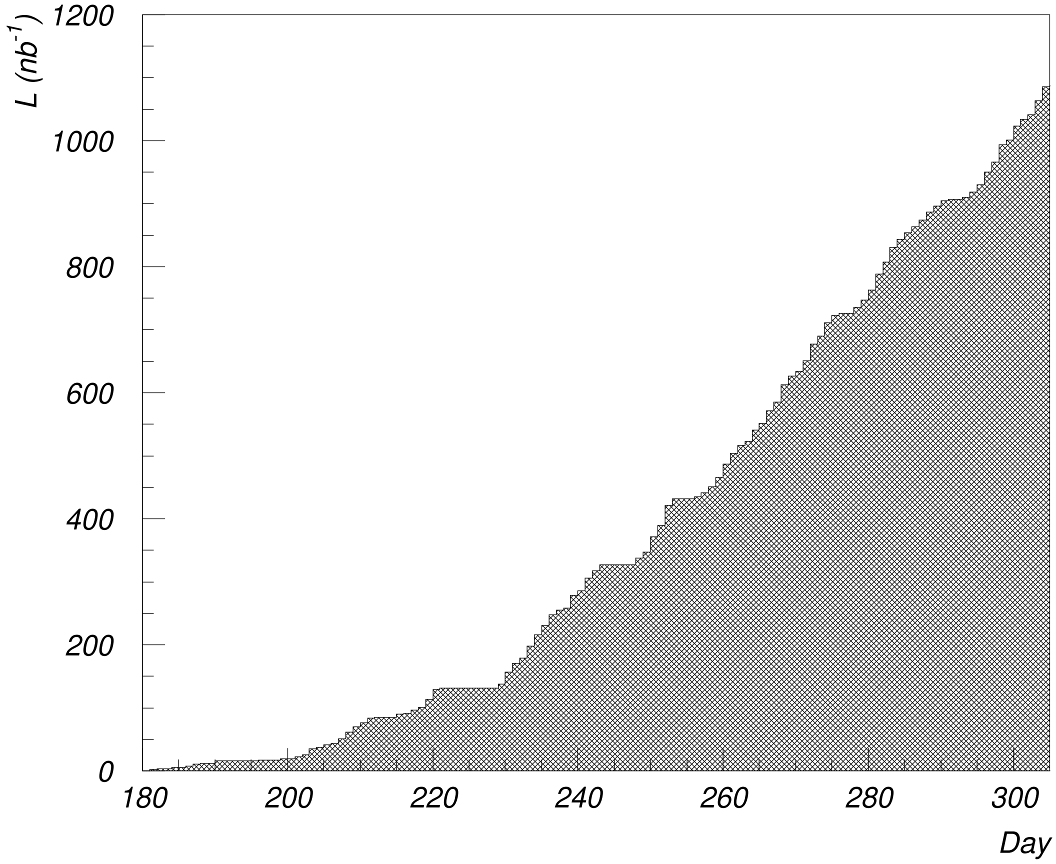

Figure 8: ZEUS on-line integrated luminosity delivered by HERA in 1993.

and in many cases the actual active time (available only offline) was much lower than the value used online.

3.4 Offline Calculations

The offline luminosity calculation is based on the analysis of data collected in the ZEUS environmental records. As was mentioned before this data contained scaler readouts both from GFLT and LUMI systems. For the luminosity determination only the following types of GFLT scalers were relevant in the offline analysis:

- counting events with $E_\gamma > 49$ ADC counts (equivalent to $E_\gamma > 5GeV$ cut for nominal calibration – duplication of the main LUMI scaler, checks data transfer to GFLT),
- counting events flagged by the LUMI hardware as luminosity events (checks operation of VME scaler),
- counting events with $E_\gamma > 28$ ADC channels ($E_\gamma > 2GeV$ with nominal calibration),
- counting events with $E_\gamma > 84$ ADC channels ($E_\gamma > 10GeV$ with nominal calibration),
- counting events with $E_\gamma > 84$ ADC channels and $E_\gamma < 127$ ADC channels ($E_\gamma > 10GeV$ and $E_\gamma < 16GeV$ with nominal calibration).

For the offline luminosity determination the measured ADC pedestal values and calorimeter calibration constants provided for each ZEUS run by another offline job (see [3]) were used in order to calculate actual threshold values. First, all energy thresholds were recalculated using the following formula:

$$T_R = \frac{T_{ADC} - P_{ADC}}{C}, \tag{6}$$

where: T_R - threshold in GeV,
T_{ADC} - threshold in ADC counts,
P_{ADC} - measured pedestal value in ADC channels,
C - calibration constant (ADC counts per GeV).

Secondly, the initial values of the σ^I_{obs} (from Tab. 1) were rescaled as follows:

$$\sigma^F_{obs} = \frac{\sigma^{T_R}_{BH}}{\sigma^{nom}_{BH}} \sigma^I_{obs}, \tag{7}$$

where:
σ^F_{obs} - corrected σ_{obs},
σ^{nom}_{BH} - theoretical bremsstrahlung cross-section for the nominal threshold,
$\sigma^{T_R}_{BH}$ - theoretical bremsstrahlung cross-section for the actual threshold.

Thirdly, the number of bremsstrahlung events between two environmental triggers (i.e. within about 16.6 s) was corrected for the $egas$ contribution and divided by $\sigma^{T_R}_{BH}$.

In addition, the center of the photon beam position in γcal was calculated with the use of the position detector data. The mean photon position - an average over ten subsequent

Table 3: Contributions to the Error of the Luminosity Measurement.

	$ep \rightarrow e'\gamma p$ rate measurement		'Observed' cross-section determination
a.	*egas* background subtraction	a.	cross-section calculation
b.	correction for multiple events	b.	acceptance correction
c.	counting errors	c.	energy scale errors
d.	dead-time correction		

environmental records - was used in order to reduce the statistical error. Then, the tilt of the electron beam (see next section) was calculated and the luminosity was corrected according to a change of the geometrical acceptance of the photon calorimeter (see Tab. 5) with respect to the MC nominal value (horizontal tilt equaled -0.15 mrad, no vertical tilt).

Finally, the luminosity values were again rescaled using the final corrections from Tab. 2.

4 Error of the Luminosity Measurement

4.1 Sources of the Systematic Errors

Since the luminosity value (see Eq.3) is determined from the ratio of the measured rate of ep bremsstrahlung events and the 'observed' cross-section, σ_{obs}, two main sources of systematic error in the luminosity measurement can be identified as shown in Tab. 3.

4.1.1 Errors in $ep \rightarrow e'\gamma p$ Rate Measurement

a. Uncertainty in *egas* background subtraction

Since a ratio of currents, k, is used in the procedure of the *egas* background subtraction (see previous section, Eq. 4), the error in the k measurement contributes to the error of the measurement of the rate of ep bremsstrahlung events and therefore to the luminosity uncertainty. There were two ways of monitoring the accuracy of the subtraction. In the first method, one used data from *egas* runs when only the e^- beam was stored in HERA and checked whether the rate of the bremsstrahlung events normalized with the bunch currents was the same for all bunches. In Fig. 9 such normalized rates are shown for several *egas* runs when the electron beam bunch structure was the same as for the HERA colliding mode (the change of the normalized rates from run to run reflects mainly the change of the rest gas pressure in a HERA beam pipe close to the IP).

For all *egas* runs a similar pattern was observed resulting in much lower normalized rates observed for a first bunch in a train of bunches. This significatly lowered the average normalized rate of pilot bunches since a pilot train contained just two bunches. The average rate in 'trains' of 10 bunches (which in physics runs collide with proton bunches) was lowered only slightly. The

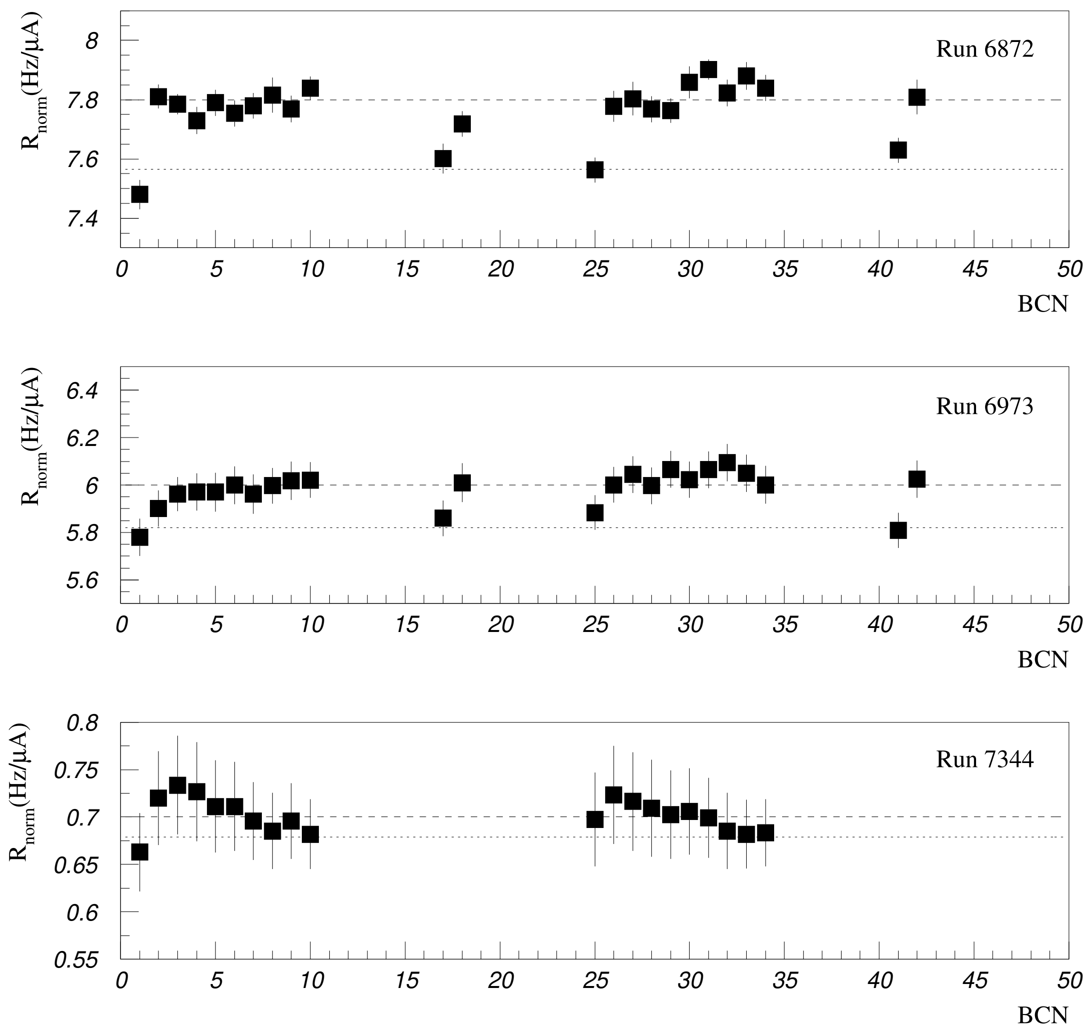

Figure 9: Mean rates, R_{norm}, of $egas$ bremsstrahlung events (with $E_\gamma > 5\ GeV$) normalized with electron bunch currents as a function of BCN for three runs when only electron beam was circulated in HERA; in run 7344 only ten bunch long 'trains' were stored and also very low rest gas pressure was observed; solid lines show an average value and dotted lines a –3% deviation from average.

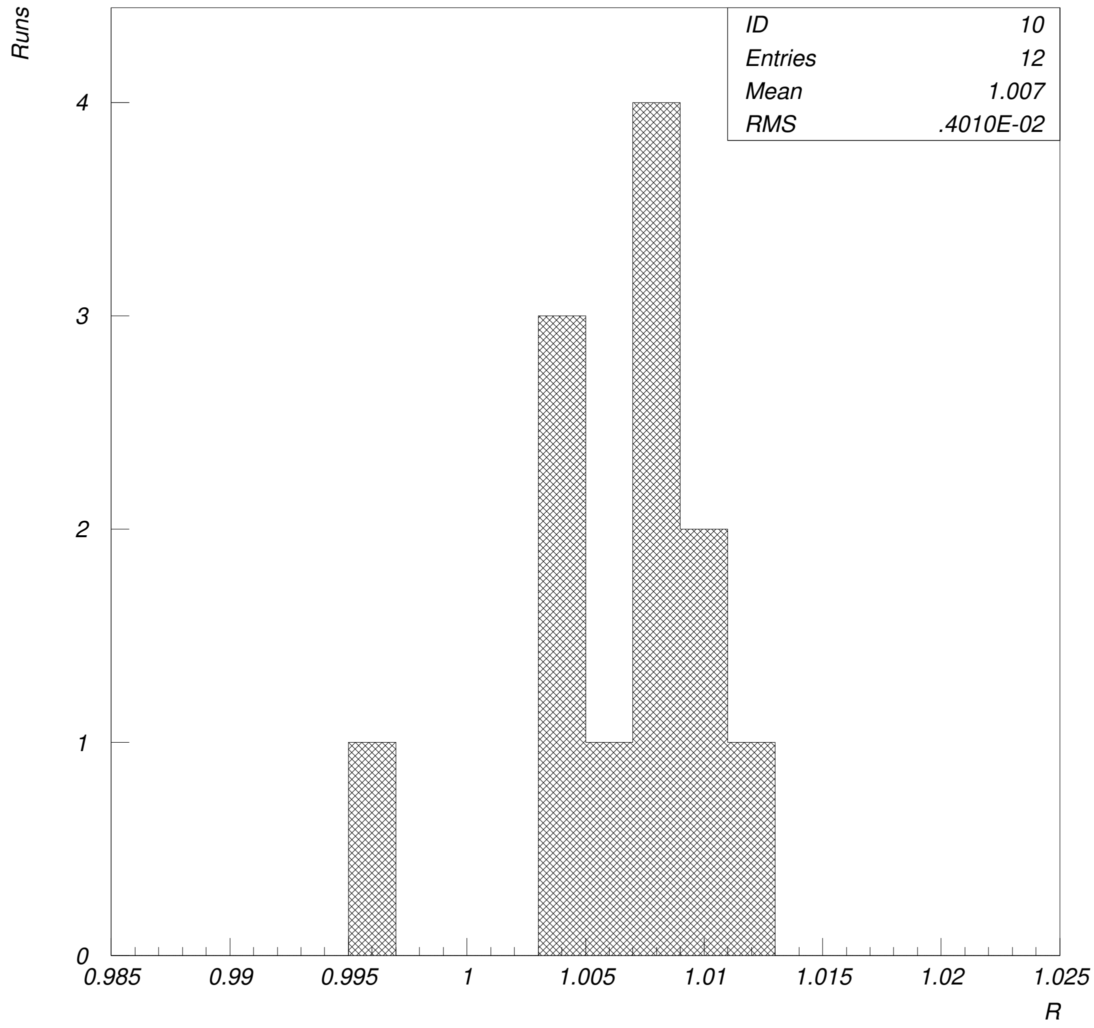

Figure 10: Distribution of the ratio, R, of normalized rates for two pairs of pilot bunches, where $R = \langle \frac{r_1^a + r_2^a}{I_1^a + I_2^a} / \frac{r_1^b + r_2^b}{I_1^b + I_2^b} \rangle$, and $r_{1,2}^{a,b}$ and $I_{1,2}^{a,b}$ are $egas$ bremsstrahlung rates and bunch currents of first and second bunch of the a and b pair, respectively.

source of the effect is unclear, however it is unlikely due to some bias in the rate measurement - all relevant parameters (as acceptance, pedestals) were the same for all bunches. May be it is caused by pileup effects in the measurements of HERA bunch currents. The typical ratio between normalized rates in these two groups of bunches (colliding vs. pilot) was 1.02. Since the average contribution of $egas$ events was 20%, this effect could result in a 0.5% underestimation of the $egas$ background contribution.

In the second method used for some large physics runs, the normalized rates from two different pairs of pilot bunches were compared. In Fig. 10 the distribution of the ratio, R, between first and second pair of pilot bunches is shown.

Both, width of the distribution of R and deviation of the average R from 1 reflect the uncertainty in the determination of the $egas$ background. But since they are much smaller ($\approx 0.5\%$) than the bias from the systematic difference between colliding and pilot bunches of 2%, therefore we neglect this uncertainty in this analysis. It results in the typical error of the subtraction of $egas$ background of 0.5% common for the on-line and off-line luminosity determination.

The error in $egas$ background subtraction could also emerge due to variation of some relevant parameters as pedestals, beam tilt, etc. with bunch crossing number. However, no significant differences were found between colliding and pilot bunches.

b. Counting errors

The counting errors can occur due to wrong flagging of the 'luminosity events' or malfuctioning of scalers which count such events. These errors were common for on-line and off-line measurement and were monitored for the nominal trigger ($E_\gamma > 5GeV$) by comparing readings from three independent scalers (see [2] for details): a VME based scaler counting the number of bremsstrahlung flags provided by so-called 'lumi_processor' (VME-flag) and two GFLT based scalers, a first one (GFLT-flag) also counting lumi_processor flags and a second one (GFLT-cut) counting flags provided by the GFLT itself. The comparison of the VME and the first GFLT scaler readings checks the functioning of both scalers and the reliability of the data transfer between VME and GFLT modules. From the comparison of the GFLT scaler readings one checks the correctness of flagging 'luminosity events'. In Fig. 11 the results of these checks are presented. In this way, the counting errors were estimated to be below 0.3%.

c. Multiple events effect

The correction for multiple events is not applied in on-line and 'nominal' off-line calculations because MC studies showed that for the main trigger ($E_\gamma > 5GeV$) this correction is negligible (see [8]). For other types of luminosity triggers corrections were applied according to results shown in the previous section (i.e. scaling the correction in Tab. 2 with the average luminosity). In Fig. 12 two plots of $\Delta L/L = (L_5 - L_{10})/L_5 \ vs. \ \langle \mathcal{L} \rangle$ are shown, before and after applying correction on pileup.

The clear dependance of 'raw' $\Delta L/L$ on the average luminosity disappears completely after correcting for multiple events. Based on this result, we estimate error due to pileup events to be below 0.2%, i.e. less than 20% $\times$ typical correction for $E_\gamma > 10GeV$ trigger.

d. Dead-time correction

The dead-time correction in the on-line measurement was quite uncertain especially when abnormal end of the data taking occured [10]. An additional uncertainty was due to averaging the correction over about 10 s. In the off-line calculations this correction was exact.

4.1.2 Uncertainty in determination of the observed cross-section

a. Theoretical cross-section

The Bethe-Heitler formula for ep high-energy bremsstrahlung which was used in calculations

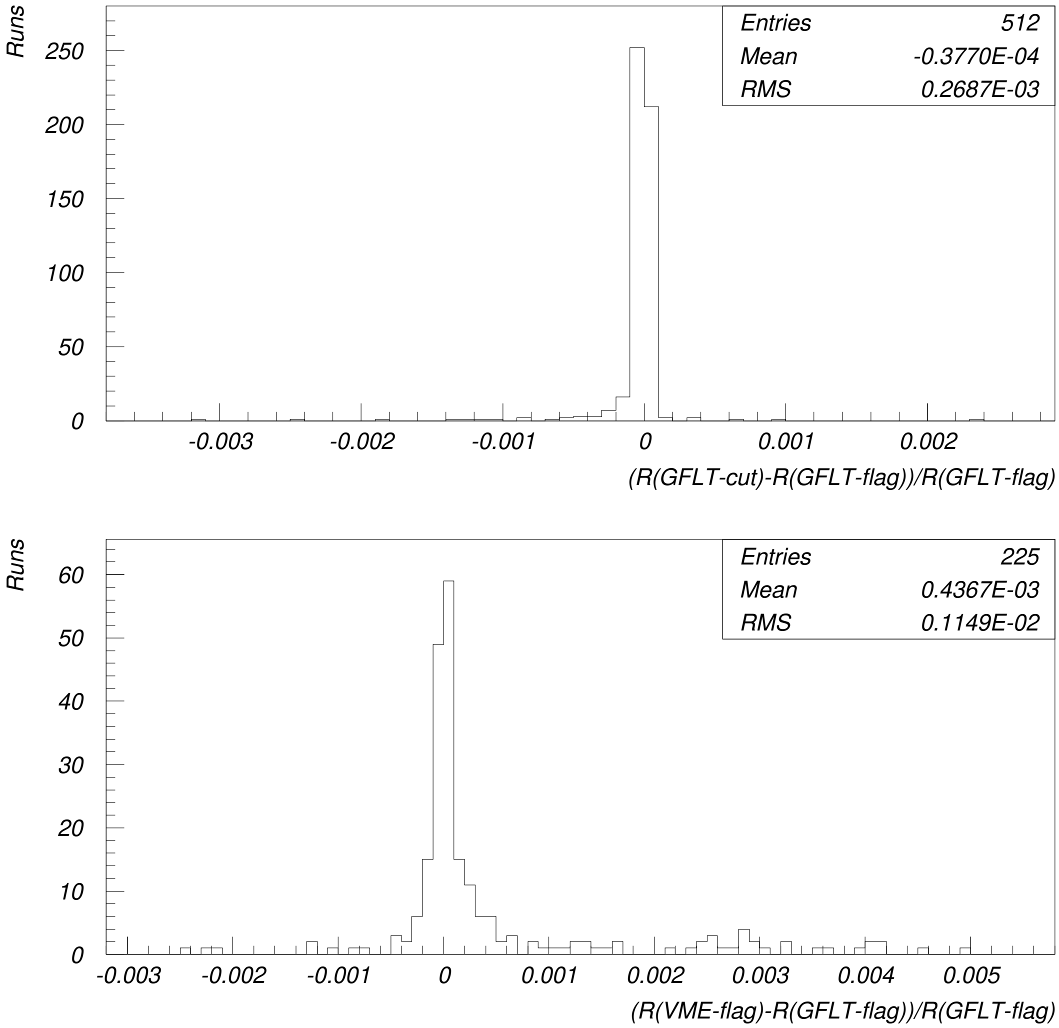

Figure 11: Distributions of relative differences between bremstrahlung counting rates (for $E_\gamma >$ $5GeV$ trigger) as measured with three independent scalers.

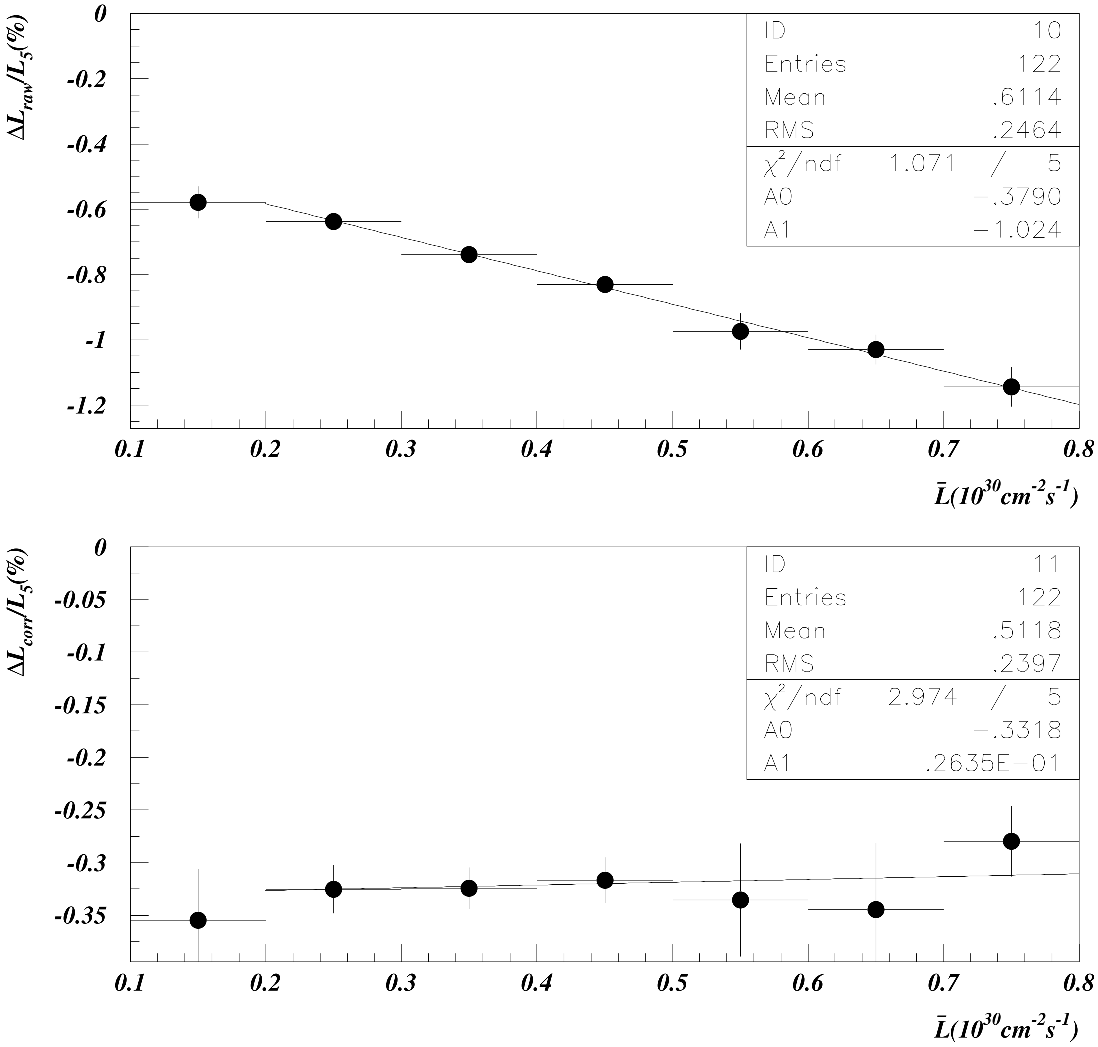

Figure 12: Relative differences, $\Delta L/L$, between integrated luminosities L_5 and L_{10} measured with $E_\gamma > 5GeV$ and $E_\gamma > 10GeV$ triggers plotted as a function of the average luminosity, before, $\Delta L_{raw}/L$ and after, $\Delta L_{corr}/L$, correction for multiple events.

Table 4: LUMI Experimental Uncertainties

Item	On-line calculation	Off-line calculation
Acceptance		
photon beam position in γcal	$\approx 0.5cm$	$< 0.1cm$
photon beam width in γcal	$\approx 0.2cm$	$< 0.1cm$
γcal position	$\pm 0.1cm$	$\pm 0.1cm$
beam-line apertures	$\pm 0.1cm$	$\pm 0.1cm$
Energy Scale		
ADC pedestals	± 1	± 0.3
ADC aperture widths	± 0.1	± 0.1
calibration constant	$\approx 4\%$	$\approx 1\%$
non-linearities	$< 0.1\%/GeV$	$< 0.1\%/GeV$
non-uniformities	$< 1\%$	$< 1\%$

of the theoretical cross-section (see Eq. [4]) was derived in the Born approximation. Higher order corrections to the Bethe-Heitler cross-section as well as corrections for the proton structure, its spin and finite mass were studied in a number of papers [11, 12, 13]. As a result one expects corrections from these sources to be less than 0.5% although some re-calculations are needed to match the actual experimental setup. The contribution from the inelastic bremsstrahlung process, $ep \rightarrow e\gamma X$, was found to be negligible [14]. However, additional corrections to the Bethe-Heitler cross-section are needed due to finite lateral sizes of HERA [7]. Since this theoretical prediction has not been tested at HERA as yet, the corrections due to the beam size effect was applied as discussed in the previous section but the total theoretical error was conservatively assumed to be 1%.

Further errors in the determination of the observed cross-section are due to uncertainty of the energy scale in the selection of 'luminosity events' and due to finite acceptance of the luminosity monitor for the detection of bremsstrahlung photons. A number of experimental uncertainties contributing to these errors are listed in Tab. 4.

b. Acceptance error

The acceptance of bremsstrahlung photons in the ZEUS luminosity monitor is in a good approximation determined only by geometry of the experimental setup, i.e. is independent of the photon energy. The reason is that the angular and the energy distributions of the bremsstrahlung photons factorize (see [15]) and practically all the energy of photons which hit the beam-line elements is absorbed and is not deposited in the calorimeter. In Fig. 13 the distribution of ratio of measured to true photon energy is shown for MC events, revealing a sharp peak at zero well separated from a broad peak at 1.0.

The acceptance depends therefore on the actual angular distribution of bremsstrahlung pho-

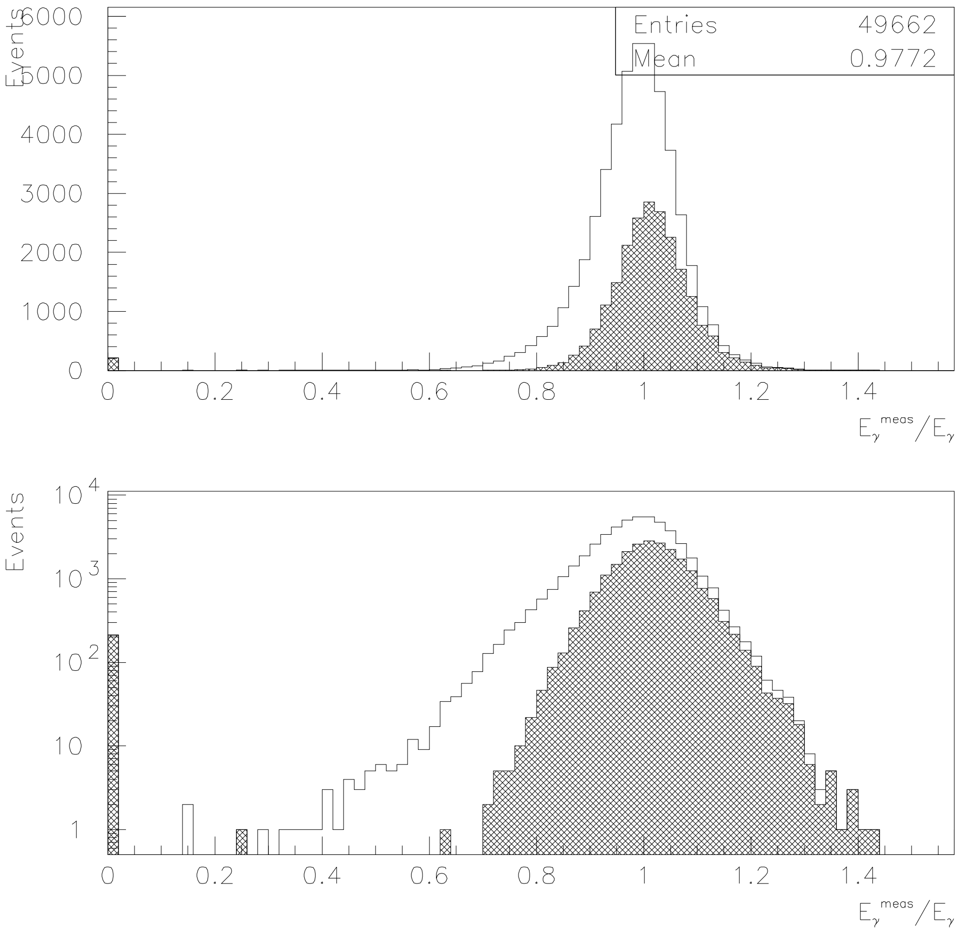

Figure 13: MC distribution of the ratio of measured, E_γ^{meas}, to generated, E_γ, energy of bremsstrahlung photons for events with $E_\gamma > 3\ GeV$; hatched histograms correspond to events when no energy was deposited in the filter in front of the γcal.

tons and the actual position of the IP [3] as well as on the positions of beam elements and detectors of the luminosity monitor. The positions of magnets and detectors were known to 1 mm and the angular distribution of bremsstrahlung photons (being a convolution of angular distribution of beam electrons at the IP with the distribution of emmision angle of bremsstrahlung photons was monitored with the use of the photon position detector.

The direction of flight of the bremsstrahlung photons was derived from the measurement of photon hit position x, y at the distance $l_\gamma = 107\ m$ from the IP, under assumption that all photons originated exactly from the IP (see remark above). The projections of the photon polar angle, θ_γ, are then calculated from:

$$\theta_\gamma^{x(y)} = x(y)/l_\gamma. \tag{8}$$

In a number of test runs when only e^- beam was circulated in HERA the details of acceptance understanding were carefully checked. For the reference, the measurements with the use of HERA beam position monitors (BPM) of the electron beam position and tilt at the IP were also performed. The BPMs used in this analysis were situated $\pm 7\ m$ from the IP and each of them consisted of four electrodes. From the asymmetry of pulses induced in the electrodes by the passing electron beam the actual beam position at that point of the HERA ring was derived. The relative accuracy of these measurements is about 0.2 mm but because the position of these detectors is known to (at most) 0.5 mm [16], the accuracy of the absolute measurement is not better than 0.7 mm. Additionally, to obtain the electron beam position and tilt at the IP from the measurements of x, y of the beam at $\pm 7\ m$ from the IP is not straightforward due to presence of two quadrupole magnets at about $\pm 6.0\ m$. From the transport matrix equations one can then derive the following formulae:

$$x(IP) = \frac{x_b + x_a}{2} c_x, \tag{9}$$

$$y(IP) = \frac{y_b + y_a}{2} c_y, \tag{10}$$

$$\theta_x(IP) = \frac{x_b - x_a}{14\ m} c_{\theta x}, \tag{11}$$

$$\theta_y(IP) = \frac{y_b - y_a}{14\ m} c_{\theta y}. \tag{12}$$

where $x(IP)$ and $y(IP)$ are respectively horizontal and vertical positions of the electron beam at the IP, $\theta_x(IP)$ and $\theta_y(IP)$ are respectively horizontal and vertical tilts of the beam at IP and x_a, x_b, y_a, y_b are measured beam positions at $\pm 7\ m$; $c_x = 0.912, c_y = 1.159, c_{\theta x} = 0.922, c_{\theta y} = 1.09$ [4]. An additional source of error enters, due to 0.5 mm uncertainty in the position of the quadrupoles. These uncertainties lead to about 1 mm and 0.1 $mrad$ errors in the determination of absolute electron beam position and tilt at the IP. In Fig. 14 the correlation between electron beam tilts measured with BPMs and γcal are shown. The error bars reflects uncertainties of the relative tilt measurement in both methods.

[3] The spatial distribution of bremsstrahlung photons at the IP has a width of the order of 0.2mm (about 0.35 mm horizontally and 0.08 mm vertically) and can be safely ignored in the acceptance considerations.

[4] In case of absence of quadrupole magnets $c_x = c_y = c_{\theta x} = c_{\theta y} = 1$.

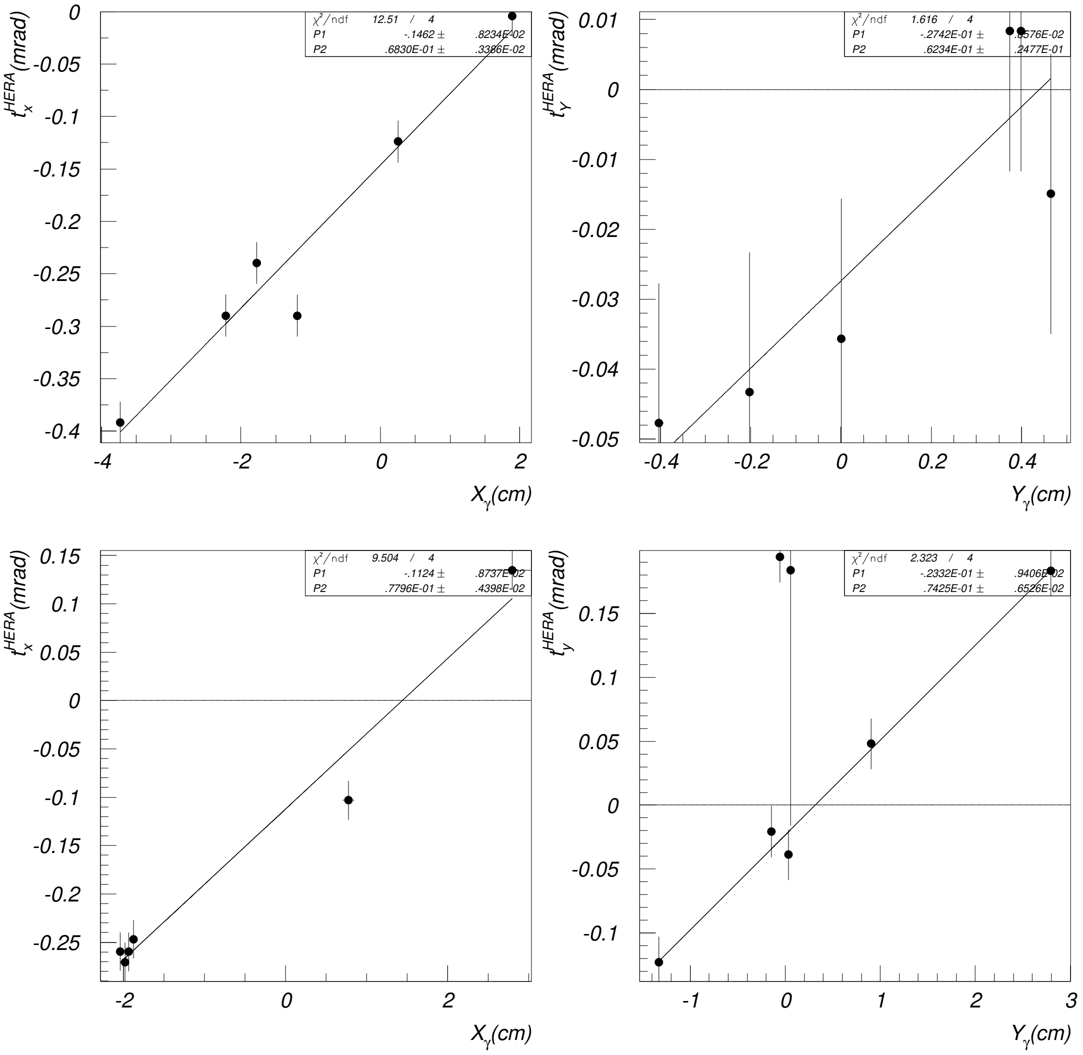

Figure 14: Comparison of BPM and γcal measurements of the (a) horizontal and (b) vertical tilts of e^- beam at the IP.

The electron beam tilts measured with both methods are well correlated but the slope in a straight-line fit in Fig. 14 is significantly smaller than 0.09 ($= 1/l_\gamma$, see Eq. 8). This may suggest some problems in calibration of BPMs close to the IP. Also value of intercept for horizontal tilts which is significantly different from zero may indicate that an axis of the two quadrupoles closest to the IP was rotated with respect to a design direction.

The full understanding of the observed discrepancies will require joint effort, both from ZEUS and HERA, and more useful data from BPMs available during regular ZEUS running period. This, however, could result in much better understanding of the beam orbits which is relevant not only for the luminosity measurement but even more for tagging photoproduction events or possibly for tracking in ZEUS in general.

Since the acceptance of bremsstrahlung photons is determined by the apertures of the beam-line magnets and shapes of the beam-pipe, the MC photon hit distributions measured with γcal were first fitted to the data from *egas* runs with large tilts of the electron beam when 'shadowing' of the photon beam by beam-line elements was large. It was done by construction of a contour being a projection of the edges of the magnet apertures onto the x-y plane at the distance of 107 m from the IP and accepting in the MC simulation only those events for which the photon position on this plane would lay within the contour. Then, after including the resolution of the position measurement in the simulation, the measured photon beam profiles were fitted by shifting the elements of the contour. In Fig. 15 several measured distributions of the photon position are compared with the MC predictions showing a good agreement. In Fig. 16 data from several runs are merged (showing in a y_γ *vs.* x_γ plot a clear shape of the acceptance boundaries) and compared with the fitted contour.

In Tab.5 value of the MC photon acceptance is listed as a function of the tilt of the electron beam at the IP. The quoted errors were found from variations of the acceptance for 2 mm shifts of the MC contour of the magnet apertures[5], and by ± 0.01 *mrad* variation of the photon beam divergence. The acceptance derived from the MC simulation was also experimentally checked with the use of a method involving bremsstrahlung tagging with the *ecal* (see [2]). The systematic uncertainties in this method were due to correction for *egas* bremsstrahlung contribution and deformation of the angular distribution of the tagged photons, and were below 0.5% for tilts below 0.5 mrad. In Fig. 17 the photon acceptance measured in this way is compared with the MC predictions showing a good agreement.

This comparison as well as the estimation of the systematic error of the acceptance prediction (see Tab. 5) showed that a 0.5% acceptance error for typical tilts of the electron beam ($-0.2 > t_x > -0.1$ *mrad* and $-0.1 > t_y > 0.1$ *mrad*) is expected.

c. Uncertainty in energy scale

The accuracy of the calibration procedure of the LUMI calorimeters was discussed in detail in [3]. The procedure was successfully tested by calibration of the MC calorimeter data and comparing the measured and 'true' calibration constants (see Fig. 18). As a result a 1% uncertainty of the photon calorimeter calibration constant was established. Such an error resulted

[5]This should include about 1 mm uncertainty of the transversal position of the IP, the 0.5 mm uncertainty in magnet positions as well as accuracy of the determination of the contour shape.

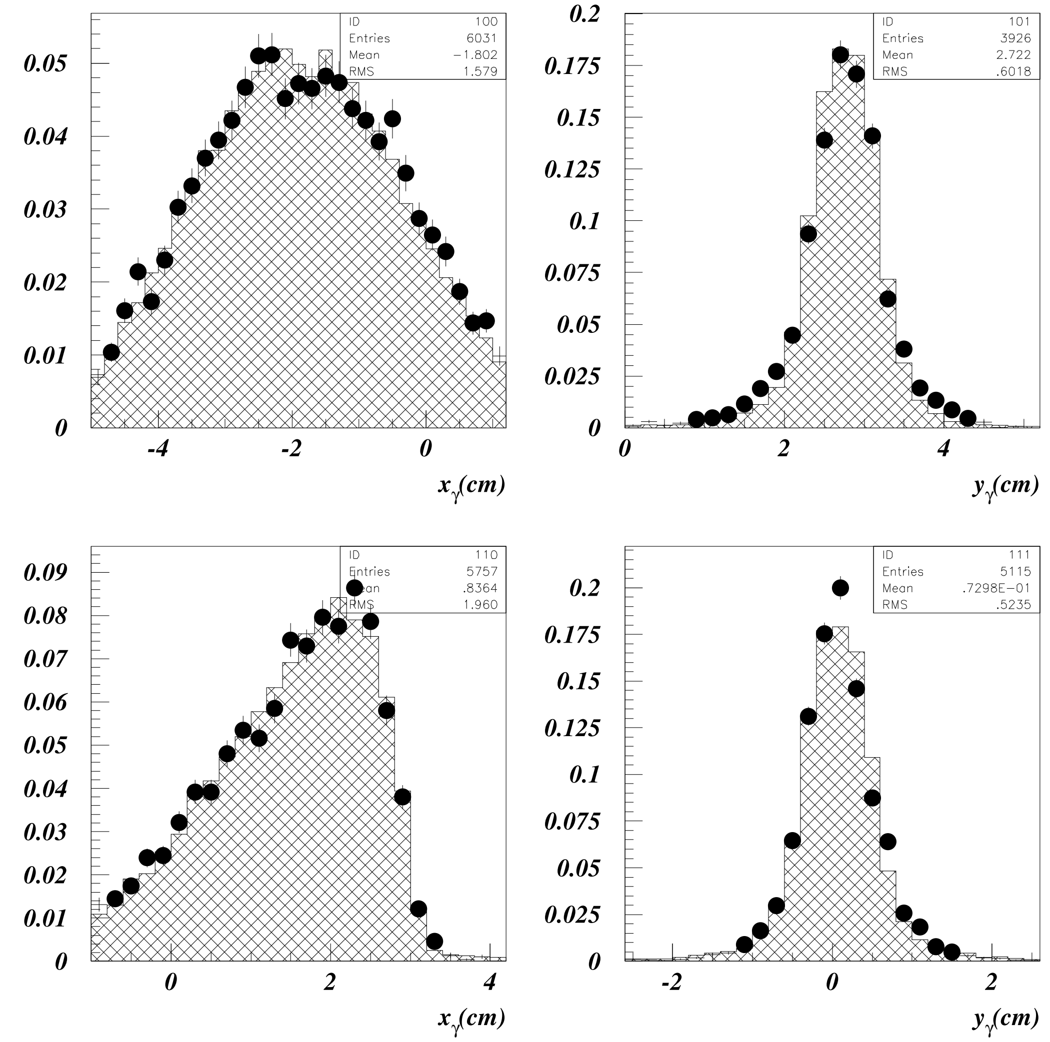

Figure 15: Comparison of the measured and simulated distributions of bremsstrahlung photon hit position for runs with large vertical (a) and horizontal (b) tilts of e^- beam at the IP.

Table 5: MC bremsstrahlung photon acceptance, A_γ^{MC}, and its error, ΔA_γ^{MC} (in brackets) as a function of e^- beam tilt (t_x, t_y) in mrad at the IP.

Tilt (mrad)	$t_x = -0.3$	-0.2	-0.1	0.0
$t_y = -0.15$	.975 (.013)	.991 (.003)	.986 (.008)	.950 (.025)
-0.10	.975 (.012)	.993 (.002)	.990 (.005)	.959 (.020)
-0.05	.975 (.013)	.993 (.003)	.991 (.004)	.961 (.019)
0.00	.975 (.013)	.993 (.002)	.990 (.005)	.962 (.017)
0.05	.974 (.013)	.993 (.003)	.990 (.005)	.959(.020)
0.10	.972 (.015)	.992 (.003)	.989 (.006)	.959 (.019)
0.15	.959 (.023)	.987 (.006)	.986 (.008)	.951 (.025)

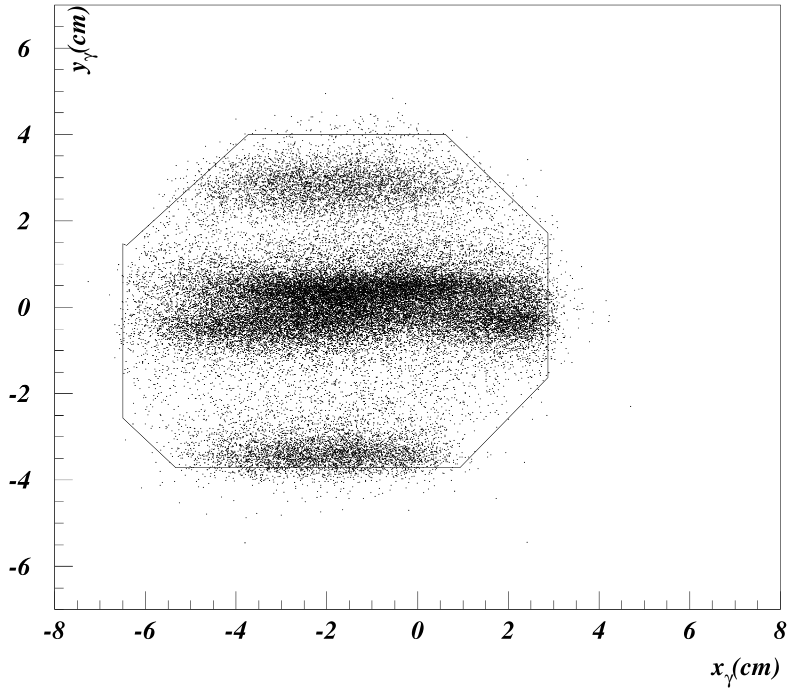

Figure 16: The measured position of photon hits in γcal merged from several test $egas$ runs with large tilts of the electron beam; also the MC contour is overlaid.

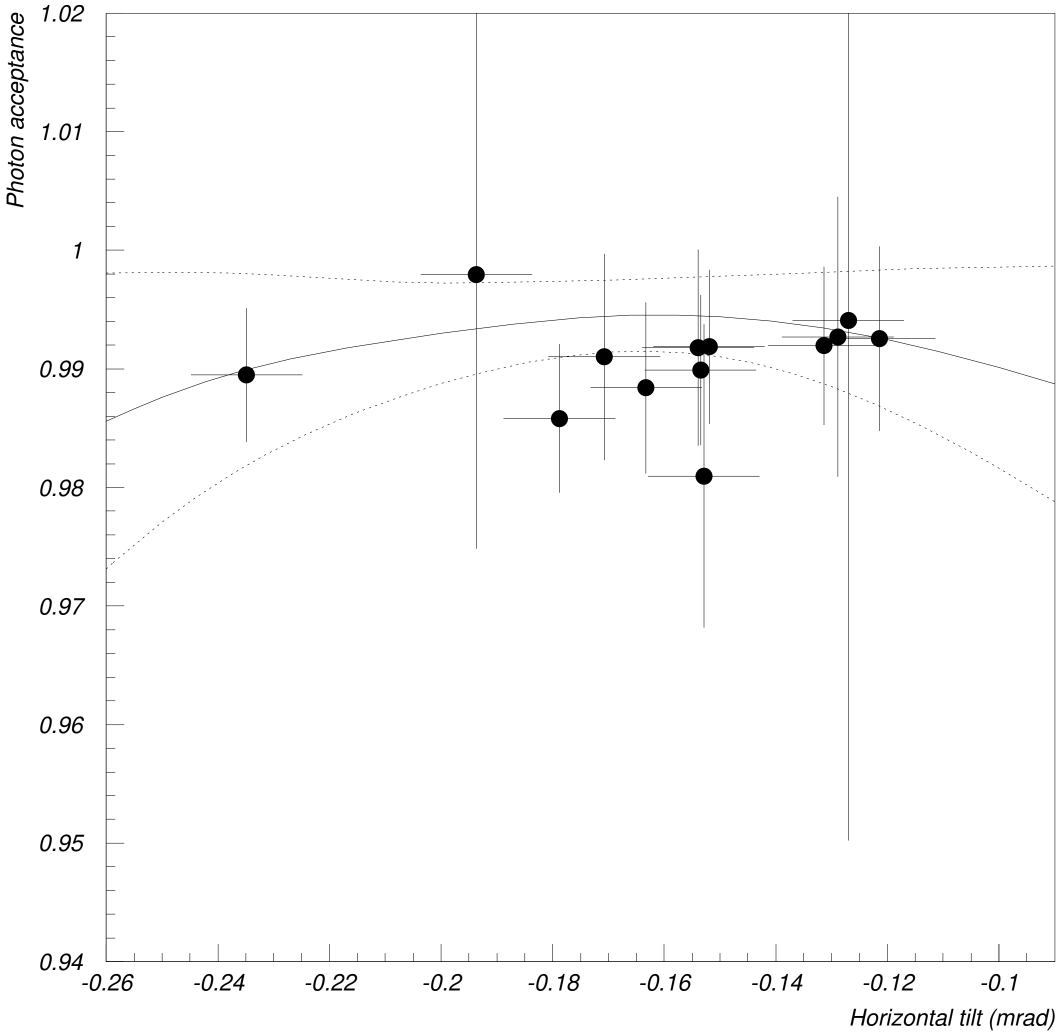

Figure 17: The measured (data points with errors) and predicted (solid line with dotted lines indicating the systematic uncertainty) photon acceptance as a function of the horizontal tilt of the e^- beam.

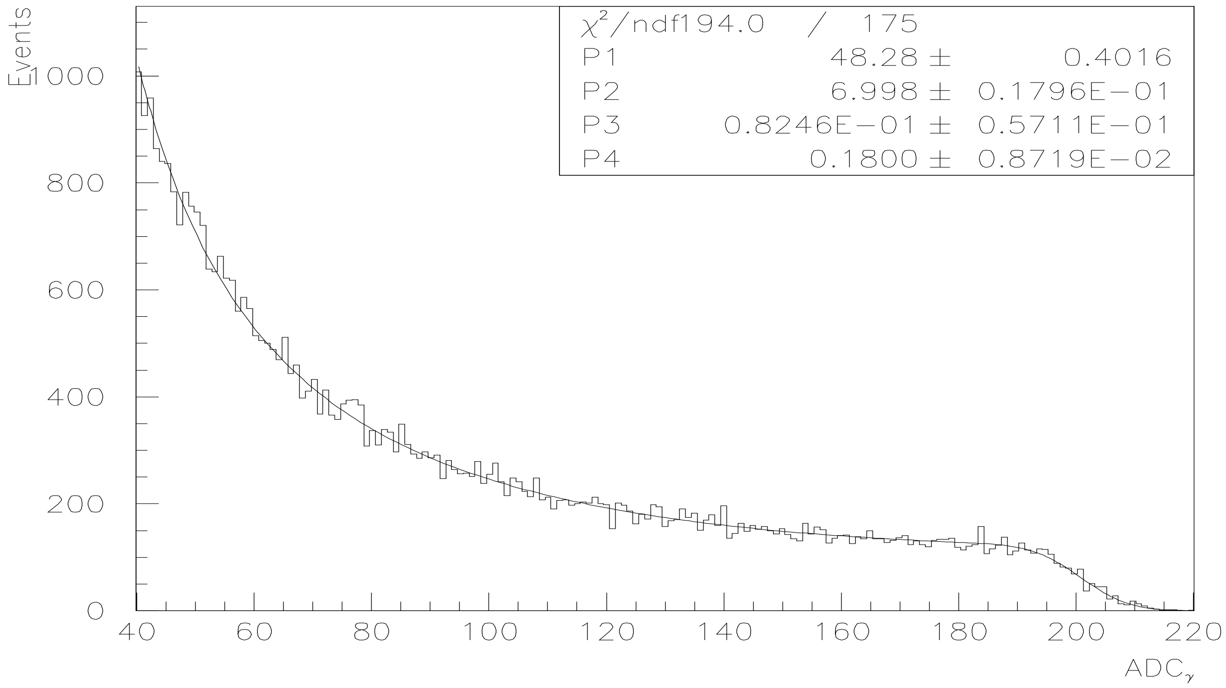

Figure 18: Calorimeter calibration fit to the MC *egas* bremsstrahlung spectrum (P1-normalization, P2-calibration constant ('true' constant equaled 7 ADC counts/GeV), P3-energy shift (in GeV) due to absorber, P4-energy resolution at 1 GeV).

in a 0.7% error in the off-line luminosity determination (where the full detector calibration was available) based on the nominal trigger [8]. The uncertainty in the on-line measurement was much higher due to large changes of the photomultiplier gains with event rate. This caused variations of the energy scale which were not corrected for and lead to an error of about 4%.

The error due to uncertainty of the photon calorimeter energy resolution $(0.22 \pm 0.02)/\sqrt{E}$ was negligible however it could slightly bias the comparison of the measured spectra with results of the MC simulation in the calibration procedure studies [3].

Since the calibration of the photon calorimeter was performed at energies close to the electron beam energy, additional non-linearities of the calorimeter and/or electronics which were not simulated in the MC could change the efficiency of triggering luminosity events. One source of the non-linearity was due to unequal apertures of FADCs used in LUMI data acquisition system (see previous section) and had to be corrected for. The correction error of ± 0.17 ADC channel was due to accuracy of the bin width measurement (≈ 0.1 ADC channel), due to usage of an average of FADC readouts rather then separate FADC counts for triggering luminosity events and uncertainty in relative contribution of two channels (≈ 0.1 ADC channel) and due to variation of ADC pedestals in time (also ≈ 0.1 ADC channel).

Another potential sources of non-linearities were the current integrators in the FADC cards, PMTs with voltage dividers or some unknown detector effects. Laboratory tests of the FADC cards [17] showed less than 1% deviations from linearity[6] in the full dynamic range. Only recently (see previous section) a $0.07\%/GeV$ non-linearity of the full calorimeter readout chain was measured. Since such a measurement was not performed in '93 running period (when different photomultipliers were used, XP2011 instead of XP2081), a 100% error was attributed to this correction. This resulted in the 1.2% contribution to systematic error of the nominal luminosity measurement.

The calorimeter non-linearity was mainly due to the presence of the carbon absorber in front of it. The MC simulation showed that for the relevant range of photon energies ($27 > E_\gamma > 2\ GeV$) the absorber decreased the average energy deposited in the γcal by about 0.27 GeV (see Fig. 19). Such a constant shift was also implemented into the fitting procedure (see Fig. 6) and improved significantly a quality of the fit. From these results we concluded that the shift of the energy deposit in the γcal due to the dead material was $0.27 \pm 0.1\ GeV$. On the other hand, the deterioration of the calorimeter energy resolution was not relevant in the luminosity measurement. No indication was found for other detector effects which could significantly affect photon energy measurement.

Additionally, the correction for mal-functioning of the data transfer to the GFLT was known to about 10%, resulting in an additional luminosity uncertainty for non-nominal luminosity triggers[7].

Errors in the pedestal determination (0.3 ADC counts) caused 0.6% and 2% errors in the nominal off- and on-line measurements respectively [8].

According to above discussion in Tab. 6 estimated 'partial' errors are collected for all luminosity triggers.

As a cross-check of the understanding of energy scale in the bremsstrahlung photon measurement the ratios of four *egas* trigger rates were compared with the MC predictions. First, the average trigger rate for each ZEUS run was normalized to the rate for the nominal trigger threshold, i.e. the rates were corrected for non-nominal calibration constants. Then, such normalized rates were compared with the MC predictions as shown in Fig. 20. The agreement was satisfactory within statistical and systematic errors. The systematic error was calculated according to the error contributions listed in Tab. 7.

4.2 On-line Luminosity Measurement

In '93 the on-line luminosity calculation involved only the subtraction of *egas* background. The nominal tilt of the electron beam (i.e. $t_x = -0.15, t_y = 0\ mrad$) and constant energy scale

[6] I.e. the maximum deviation from a straight-line fit was smaller than 1%.

[7] The nominal trigger was not affected by this bug.

[8] Due to a bug in the calibration job all pedestals for runs below 6100 (corresponding to 3.5% of the integrated luminosity) had to be lowered by one ADC count.

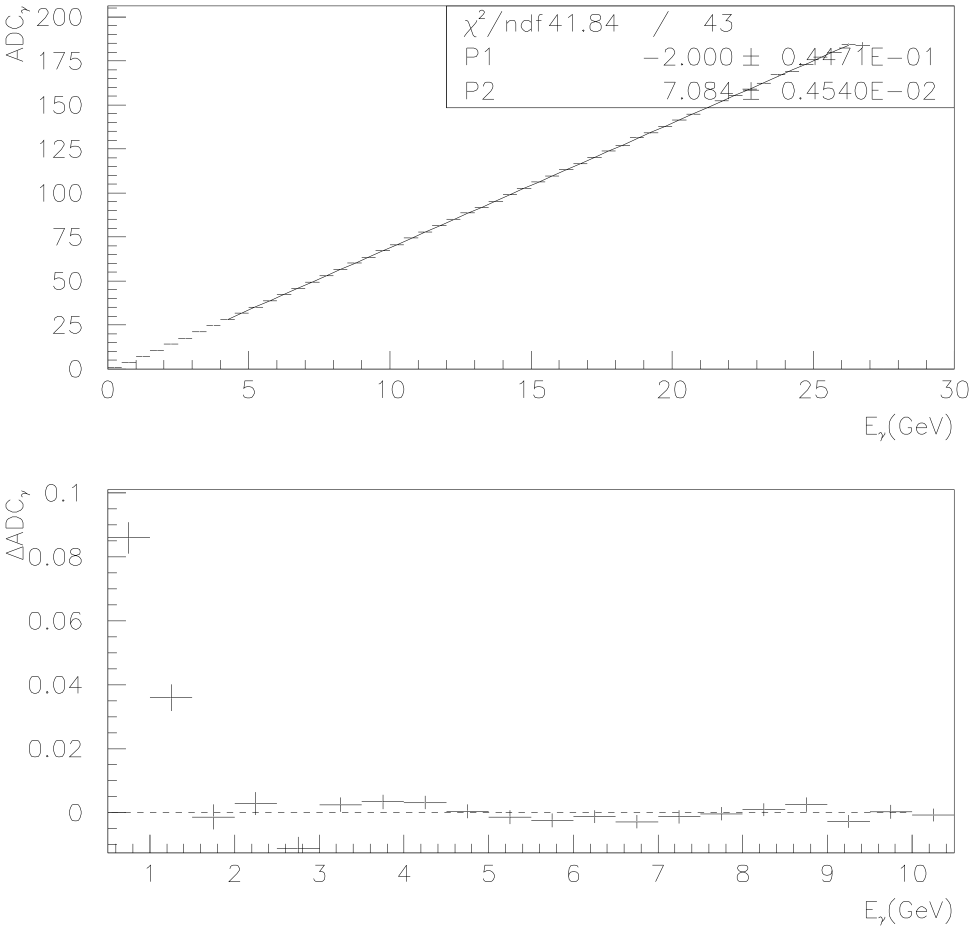

Figure 19: Average ADC count as a function of the generated photon energy, E_γ , for the MC sample used in the luminosity analysis; a straight-line fit has a non-zero intercept value (P1 parameter) corresponding to about 0.27 GeV shift of the measured energy for photon energies above 2 GeV; in the lower plot the relative difference, ΔADC_γ, between the fit and data is shown as a function of E_γ.

Table 6: Luminosity uncertainty (in per cent) due to various experimental errors for all luminosity trigger types

Error type	Trigger type			
	$E_\gamma > 2GeV$	$E_\gamma > 5GeV$	$E_\gamma > 10GeV$	$16 > E_\gamma > 10GeV$
Calibration constant	0.5	0.7	1.1	0.2
FADC threshold value	0.55	0.35	0.25	0.2
Pedestal uncertainty	1.0	0.6	0.5	0.4
Non-linearity in electronics	0.95	1.2	1.4	1.3
Calorimeter non-linearity	2.3	1.4	1.1	1.2
GFLT data bug	0.35	–	0.2	0.15
Total error	2.8	2.1	2.2	1.9

Table 7: Systematic errors (in per cent) in the mesurement of the ratios of the $egas$ rates.

Error contribution	$R_{5/2}$ $\frac{Rate(E_\gamma>5GeV)}{Rate(E_\gamma>2GeV)}$	$R_{5/10}$ $\frac{Rate(E_\gamma>5GeV)}{Rate(E_\gamma>10GeV)}$	$R_{5/10-16}$ $\frac{Rate(E_\gamma>5GeV)}{Rate(16>E_\gamma>10GeV)}$
Calibration constant	0.23	0.40	0.50
FADC threshold value	0.38	0.11	0.15
Pedestal uncertainty	0.38	0.11	0.15
Non-linearity in electronics	0.26	0.24	0.02
Calorimeter non-linearity	0.89	0.26	0.35
GFLT data bug	0.13	0.04	0.05
Total systematic error	1.10	0.56	0.65

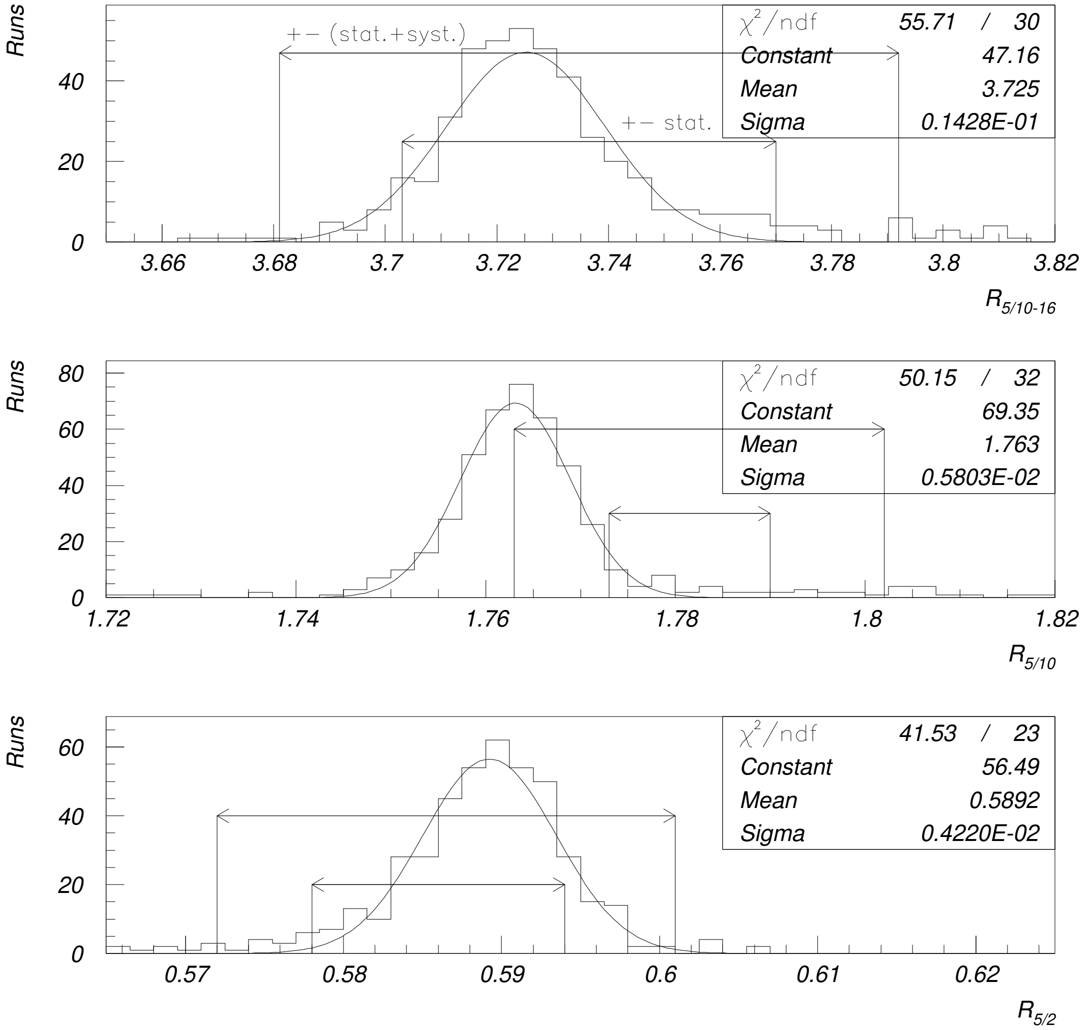

Figure 20: Distribution of the ratios of the *egas* bremsstrahlung rates normalized to the nominal threshold values for runs (#> 6100 -no pedestal bug); also the statistical and systematic errors are indicated for the MC predictions of 3.736, 1.782, 0.586 respectively.

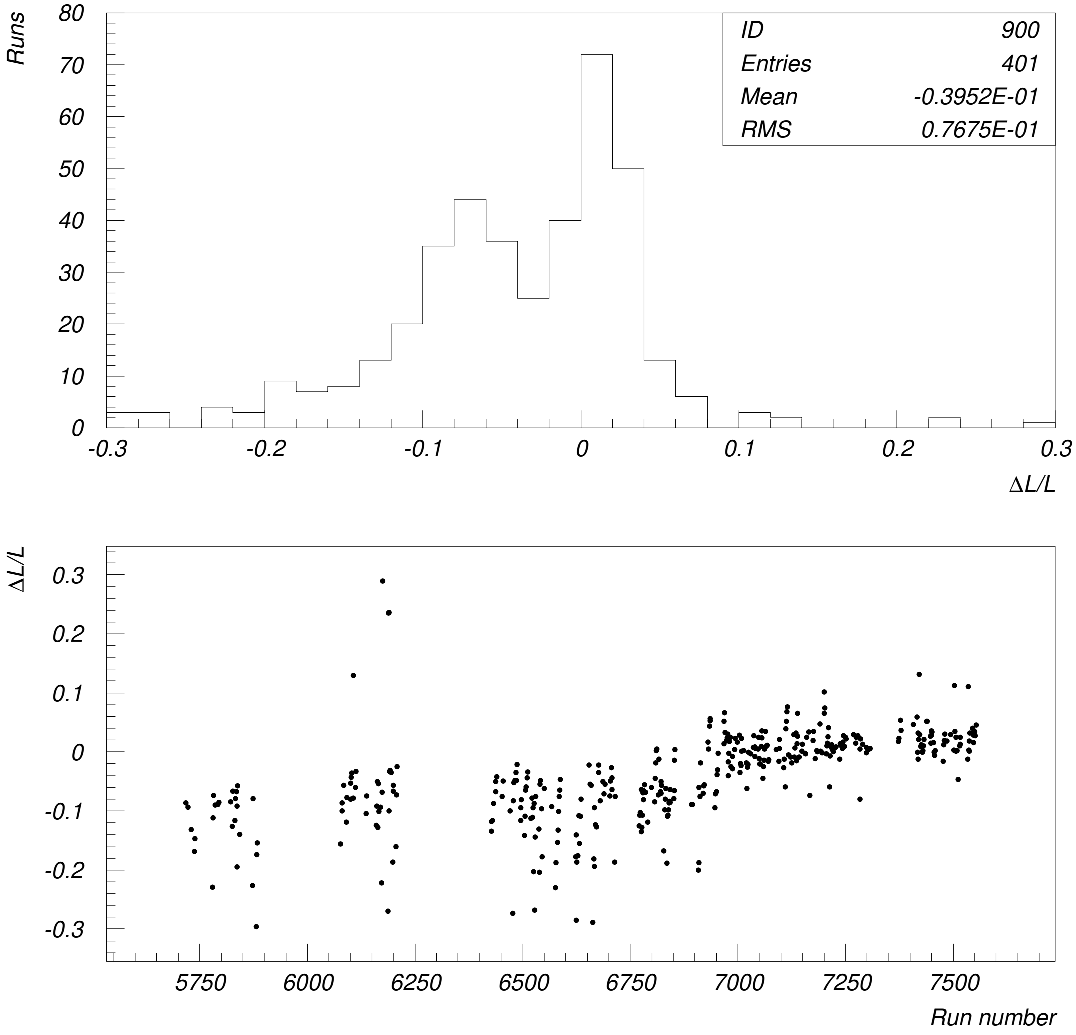

Figure 21: The distribution of the relative difference between online and offline integrated luminosities, $\Delta L/L$, and its history for all ZEUS runs with integrated luminosity larger than $100\ \mu b^{-1}$ (note a jump due to the change of the PMT HV, visible in the lower plot around run 6900).

(no correction for pedestal shifts and variation of the γcal calibration constants) were assumed. In Fig. 21 the relative difference between integrated luminosities calculated online and offline are shown, separately before and after dead-time correction. If one assumes that the offline measurement is much more accurate than the online one, then the widths of these distributions directly reflect the error of the latter.

It was clear that when high dead-time conditions occured it seriously deteriorated the accuracy of the on-line measurement and became biggest source of uncertainty in the on-line measurement.

4.3 Off-line Luminosity Measurement

The offline luminosity determination in '93 involved a number of corrections described in Sec. 3. According to the discussion of in Sec. 4.1, the contributions to the systematic error of the

Table 8: Systematic error of the luminosity measurement in '93.

Contribution	Trigger type			
	$E_\gamma > 2GeV$	$E_\gamma > 5GeV$	$E_\gamma > 10GeV$	$16 > E_\gamma > 10GeV$
$egas$ background subtraction	0.5%	0.5%	0.5%	0.5%
Correction for multiple events	0.1%	0.1%	0.1%	0.05%
Counting errors	$\approx 0.3\%$	0.3%	$\approx 0.3\%$	$\approx 0.3\%$
Cross-section calculation	1.5%	1.0%	0.7%	1.0%
Acceptance correction	0.5%	0.5%	0.5%	0.5%
Energy scale errors	2.8%	2.1%	2.2%	1.9%
MC statistics	0.6%	0.6%	0.7%	1.0%
Total systematic error	3.3%	2.6%	2.5%	2.5%

luminosity measurement can be summarized as shown in Tab. 8. Since all contributions are independent on one another, therefore errors can be summed up in quadrature resulting in a 2.5% total systematic error of the ZEUS luminosity measurement.

In Fig. 22 the nominal luminosity is compared with the luminosities measured with three other trigger setups. The average and width of the distribution of the relative difference between them is a measure of the luminosity errors except common ones (as acceptance and, possibly, counting as well as $egas$ background subtraction errors). The contributions to the systematic error were taken from Tab. 7 (difference between $egas$ and ep bremsstrahlung is here negligible) with the additional errors due to the beam-size effect and corrections for multiple-events. The comparison shows that all measurements are consistent within systematic and statistical (due to MC limited sample) errors.

4.4 Conclusions

A comparison of the present analysis with the study of systematic errors of the luminosity measurement in '92 running period [2] shows that much of the improvement in the accuracy (from 4.5% to 2.5%) was achieved thanks to:

- better understanding of photon acceptance (reliable tool for monitoring it) – error decreased from 2.0% to 0.5%,
- smaller $egas$ background and more reliable method of subtraction – error decreased from 2.0% to 0.5%,
- some improvements in measurement of photon energy (new vaccum pipe and moving absorber towards γcal) and in simulation of electronics (correcting for FADC bin widths) – error decreased from 2.5% to 2%.

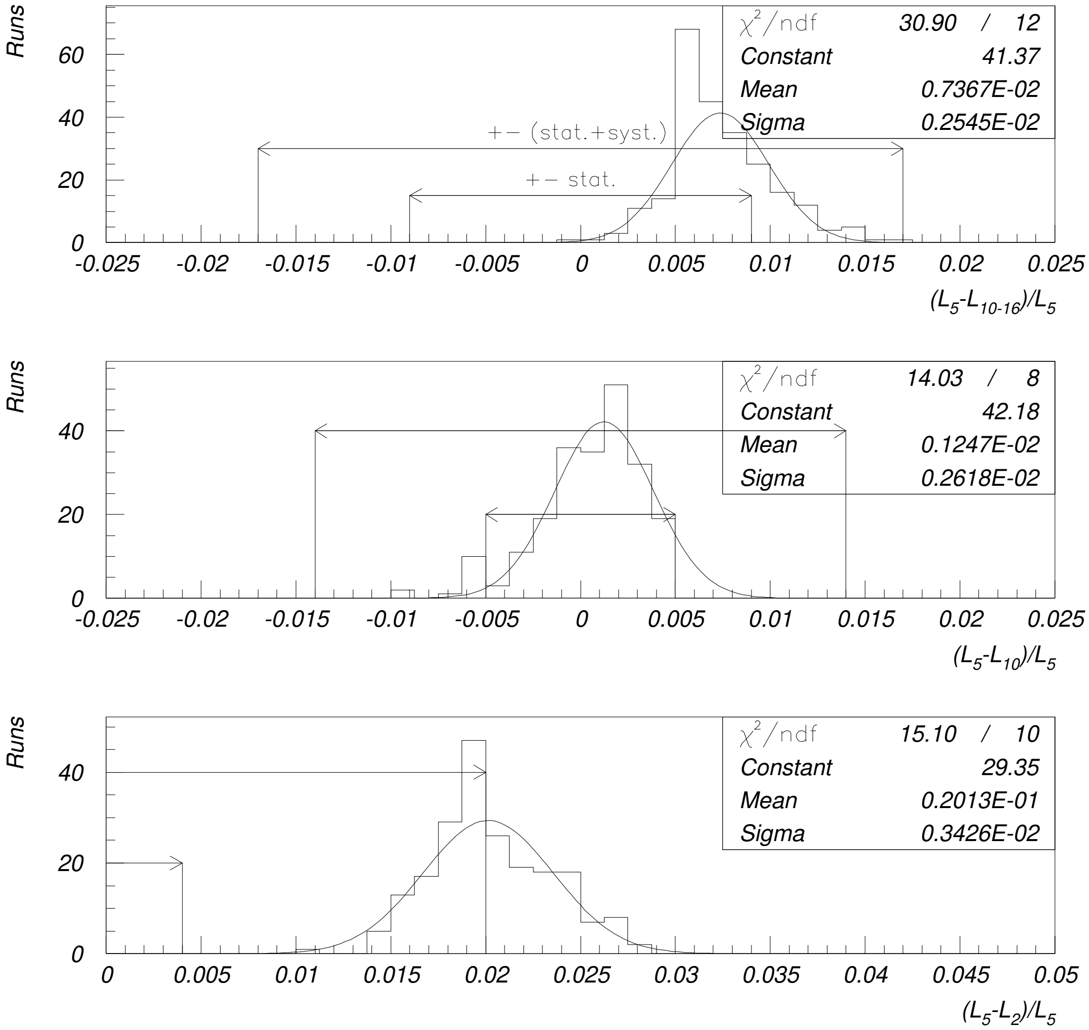

Figure 22: Distribution of the relative differences between nominal luminosity, L_5 ($E_\gamma > 5GeV$ trigger), and three other luminosities, L_2, L_{10} and L_{10-16} (with $E_\gamma > 2, E_\gamma > 10$ and $16 > E_\gamma > 10GeV$ triggers, respectively); also statistical and systematic errors are indicated.

This clearly indicates that further improvement of the precision will require better understanding of photon energy measurement. Also much larger MC data samples (at least ten times) will be needed. To provide better on-line luminosity measurement one additionally needs to ensure much more accurate correction for dead-time in the ZEUS DAQ system.

5 Outlook

The experience of running luminosity monitor in '93 and error analysis show that further improvements of the luminosity measurement can be only achieved by better understanding of the energy scale in the photon measurement and by reducing theoretical uncertainties in the cross-section calculations. The stability of the PMT gains seems to be now maintained at acceptable level by the new calorimeter PMTs as experience from '94 running period shows. Also a method of monitoring non-linearity in electronics was developed in '94. Further reduction of the energy scale error can be possibly performed by design of a new photon calorimeter and readout electronics which is planned for '95. In this context also better radiation hardness of the photon detector should be considered as to avoid such problems at all, especially for there is no precise way to control effects of the radiation damages in the LUMI calorimeters[9]. There is also hope that in a near future the problem of corrections due to beam size effect, being now the source of the biggest theoretical uncertainty, will be resolved. Then, further progress needs much work of re-calculating all theoretical corrections for the actual experimental setup of the ZEUS luminosity monitor. This, under all above conditions, makes us belive that $\approx 1\%$ accuracy of the luminosity measurement in '96 is feasible.

The development of the on-line luminosity measurement is an another line of progress. The aim is to achieve target accuracy already on-line, leaving for off-line analysis only checks of the quality of data, cross-checks of on-line results, etc. A significant progress was already achieved in '94 running period by including the acceptance and pedestal correction in on-line algorithms. In '95 there are plans of including in on-line measurement also corrections for the PMT gains and for ZEUS dead-time in the DAQ system.

6 Acknowledgements

We would like to thank very much Dr. Robert Klanner for the critical reading of the draft of this note and for many useful comments and suggestions.

[9]The radiation damage is localized in a small volume around the region of the maximum shower deposit.

References

[1] J. Andruszków et al., *First Measurements of HERA Luminosity by ZEUS Lumi Monitor* , DESY 92-066, May 1992.

[2] K. Piotrzkowski, *Experimental Aspects of the Luminosity Measurement in the ZEUS Experiment*, DESY-F35D-93-06, Oct 1993, Ph.D. Thesis.

[3] J. Andruszków et al., *Calibration Procedure of the Calorimeters of the ZEUS Luminosity Monitor*, ZEUS-Note 94-071.

[4] H. Bethe and W. Heitler, Proc. Roy. Soc. **A146** (1934) 83.

[5] M. Przybycień, *BREMLU 1.0 - Generator for LUMI*, ZEUS-Note 93-079;
K. Piotrzkowski, L. Suszycki, *BREMGE, A Monte Carlo Generator of High Energy Electron-Proton and Electron-Nucleus Bremsstrahlung Events*, Proc. of the Workshop, Physics at HERA, Vol.3, 1463-1467, Hamburg, October 1991.

[6] L. Adamczyk, private communication.

[7] G.L. Kotkin, V.G. Serbo and A. Schiller, Int. J. Mod. Phys. **A7** (1992) 4707-4745.

[8] K. Piotrzkowski, *Optimization of the Luminosity Measurement*, ZEUS-Note 94-072.

[9] K. Piotrzkowski, LUMI weekly meeting, December 1994.

[10] K. Tokushuku, private communication.

[11] K.J.F. Gaemers, M. van der Horst, Nucl. Phys. **B316** (1989) 269; erratum, ibid. **B336** (1990) 184.

[12] A.A. Akhundov, D.Yu. Bardin and L.V. Kalinovskaya, Zeit. f. Phys. **C51** (1991) 557.

[13] M. van der Horst, Nucl. Phys. **B347** (1990) 149.

[14] M. van der Horst, Phys. Lett. **B244** (1990) 107.

[15] V.B. Berestetskii, E.M. Lifshitz and L.P. Pitaevskii, *Quantum Electrodynamics*, Oxford, Pergamon Press, 2nd ed., 1982.

[16] W. Bialowons, private communication.

[17] P. Jurkiewicz and A. Kotarba, LUMI weekly meeting, July 1993.